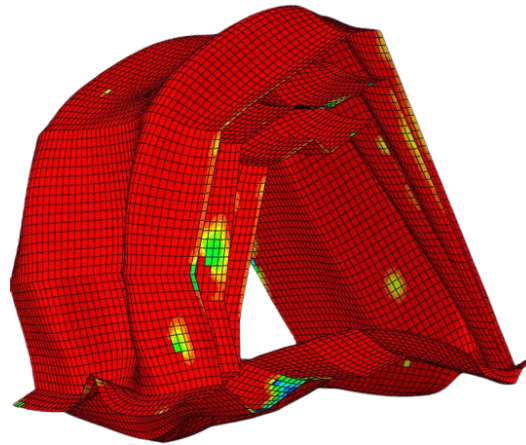




JÖNKÖPING UNIVERSITY
School of Engineering

Correlation-based analysis on thin walled tubes.



Authors: *Andreas Hedlund & Daniel Blom*
Department: *School of Engineering*
University: *Jönköpings University*
Country: *Sweden*
Date: *August 2022*

Acknowledgement

We would like to give a special thanks to Mohammad Arjomandi Rad who has been a great supervisor to us, always ready to help and steer us in the right direction. We would also like to thank Jönköping university for giving us the opportunity to conduct this thesis.

Examiner: *Roland Stolt*

Supervisor: *Mohammad Arjomandi Rad*

Scope: *30 Credits*

Abstract

In the transportation sector, crash structures are often used to protect their inhabitants in the event of a collision. These crash structures frequently utilize thin-walled tubes as energy absorbers. The process of developing thin-walled tubes is iterative based and requires multiple simulations, making it resource intensive. This thesis researches how thin-walled tubes are developed today, what kind of challenges exist in the development process and what tools and methods are used to shorten the development lead times. Later a new method for assessing TWBs crashworthiness before a simulation is investigated. In this method 43 cross-section geometries from thin-walled tubes used in automobiles are parameterized. These tubes are later subjected to a dynamic crash simulation along their longitudinal axis. Results from these simulations are correlated to their respective parameters in order to find meaningful relation between the parameters and results. It was found that the circumference of a cross-section correlates with its crashworthiness. With this finding, the development lead times of thin-walled tubes could be shortened by reducing the amount of required FEM simulations.

Keywords: Thin-walled tubes, Crashworthiness, Energy absorption, Finite element method, Finite element method automation.

Acronyms

FEM	Finite element method
FEA	Finite element analysis
SEA	Specific energy absorption
CAD	Computer-aided design
CAE	Computer-aided engineering
TWB	Thin walled beams
BC	Boundary condition
CFE	Crash force efficiency
PCF	Peak crush force
MCF	Mean crush force

Nomenclature

P_{max}	Peak crush force
E	Elastic modulus
ξ	Fraction of critical damping
ρ	Density
A	Area
J	Joules
m	Mass
ω_{max}	Highest frequency
L^e	Element length
C_d	Wave speed in the material
t_{stable}	Stability limit

Contents

1	Introduction	1
1.1	Iterative design process	2
1.2	V-Model	3
1.3	Simulation driven design	3
1.4	Problem description	4
1.5	Research question	4
1.6	Delimitations	5
1.7	Troubles during thesis	6
2	Literature review	7
3	Theory	9
3.1	Thin walled tubes	9
3.2	Energy absorption	10
3.2.1	Peak crush force	10
3.2.2	Total energy	11
3.2.3	Mean crush force	11
3.2.4	Specific energy absorption	11
3.3	Energy absorptions in automobiles.	11
3.3.1	Unibody	12
3.3.2	Materials	12
3.4	Mesh	13
3.5	Mass Scaling	13
3.6	Python	14
3.7	Automation	14
3.8	Parametrization	15
3.9	Medial Axis	15
4	Methodology	16
4.1	Cross-section geometries	16
4.2	Studied case	18
4.3	Finite element automation	22
4.4	Feature extraction	25
4.4.1	Rhino Grasshopper	25
4.4.2	Circumference	26
4.4.3	Area	26
4.4.4	Medial Axis	27
4.4.5	M/C ratio	29
4.5	Verification data	30
4.5.1	Material Model	30
4.5.2	Verified Geometry	30
4.5.3	Test rig arrangement	31
4.5.4	Mesh convergence study	32
4.5.5	FEM validation results	33

5	Results	34
5.1	Cross-section geometries	34
5.2	Geometrical parameter values	39
5.3	Simulation results	40
5.4	Correlation studies	41
5.4.1	Circumference	41
5.4.2	Medial axis length	42
5.4.3	Area	43
5.4.4	M/C ratio	44
6	Discussion	46
6.1	Research question 1	46
6.2	Research question 2	46
6.3	Research question 3	46
6.4	Method/Results	46
6.5	Further research	47
7	Conclusion	48

List of Figures

1	An example of a car frame, note the many different TWBs geometries [1] . . .	1
2	An example of an iterative design process.	2
3	V-Model (Modified from source: Experimental Dynamic Substructuring: Analysis and design strategies for vehicle development [2])	3
4	The figure visualizes three plates(Indicated by numbers 1, 2, and 3), and the arrows point at the welds between the plates.	5
5	A typical design process for TWBs [3].	7
6	An example of a geometry before the optimization process is executed [4]. . .	8
7	Example of global (b) and local buckling (a), in the corresponding load displacement graph (c)[5]	9
8	Thin walled tube with aluminum foam as filler material [6]	10
9	Example of a load-displacement graph	10
10	Stiffness compared to strength [7]	12
11	Example of a parameterized 2d geometry	15
12	Example of a geometry with a medial axis [8],	15
13	Car frame with beams [9].	16
14	Beams 46 coordinates in the order that they have been recorded, see the table 2.	17
15	Picture of extrude geometry 33.	18
16	Picture of the boundary condition applied to geometry 33.	19
17	A picture of a fished mesh, geometry 33.	20
18	The visual representation of the Rhino grasshopper code.	25
19	Geometry with circumference (black)	26
20	Total area of the geometry	26
21	The imported points in Rhino, The constructed lines from the imported points in Rhino.	27
22	The circumference divided into multiple points	27
23	The geometry after the Voronoi operation.	28
24	Cleaned geometry showing the medial line in one of the cells	28
25	The geometry after the second medial line has been calculated	29
26	A6060 T5 Engineering Strain	30
27	Test specimen geometry [5]	31
28	Test rig arrangement [5]	31
29	Peak and mean crush force compared to mesh size	32
30	Total displacement and simulation time compared to mesh size	32
31	Experimental result of DRA11 compared to the simulated result	33
32	All 46 Cross-section geometries.	38
33	Peak crush force and SEA compared to circumference for 1 mm thickness. . .	41
34	Peak crush force and SEA compared to circumference for 2 mm thickness. . .	42
35	Peak crush force and SEA compared to circumference for 3 mm thickness. . .	42
36	Peak crush force and SEA compared to medial axis length for 1 mm thickness. .	42
37	Peak crush force and SEA compared to medial axis length for 2 mm thickness. .	43
38	Peak crush force and SEA compared to medial axis length for 3 mm thickness. .	43
39	Peak crush force and SEA compared to area for 1 mm thickness.	43
40	Peak crush force and SEA compared to area for 2 mm thickness.	44
41	Peak crush force and SEA compared to area for 3 mm thickness.	44

42	Peak crush force and SEA compared to the M/C ratio for 1 mm thickness.	. 44
43	Peak crush force and SEA compared to the M/C ratio for 2 mm thickness.	. 45
44	Peak crush force and SEA compared to the M/C ratio for 3 mm thickness.	. 45

List of Tables

2	Beams 46 coordinates recorded in sheet based on the figure 14.	17
3	Analytical wall properties	18
4	An example of a geometry 45 being crushed with 4 different time steps, the beam is seen from the front and top.	21
5	Variables	22
6	Material Data	30
7	Experimental test data	32
8	Experimental test results	32
9	FEM validation results	33
10	FEM validation error rates	33
11	The calculated values for each parameter	39
12	FEM results for each geometry and thickness	40
13	Correlation R^2 values for peak crush force	41
14	Correlation R^2 values for specific energy absorption	41

1 Introduction

Since automobiles and other transport methods have flourished where people are transported inside a structure at high speeds much research effort has been devoted to making these structures safer. Safety features that today seem obvious such as laminated glass, seat belts, and crumple zones took, in reality, a long time to be developed and adapted.

The first high-speed impact testing was done in 1934 by GM while the first crumple zone concept took another 21 years to be patented. Crumple zones and energy absorption ability remain one of the most important safety features in cars today. Crumple zones work by converting the kinetic energy observed during impact into other forms of energy and increasing the amount of time the occupants are subjected to the change in momentum. This ability of a structure to absorb force is known as crashworthiness.

Thin-walled tubes are a hotspot for research when it comes to energy absorption, because of their lightweight, low cost, and frequent use in the industry. Many different characteristics of thin-walled tubes have been researched such as: taper angles, different cross-section designs, multiple cells, corrugated structure, and the use of foam as filler material.

Automakers prioritize efforts into reducing the overall weight of their vehicles, heavier automobiles have greater inertia and rolling resistance which contributes to higher fuel consumption. The main structure of a car before mounting of motor, seats, electronics, etc. is known as body in white (BIW). This is where the main energy absorbers are located. The BIW accounts for 30%-40% [10] of a car's total weight, therefore the need to develop low-weight energy absorbers. The BIW of an automobile consists of multiple TWBs, each TWB is designed to absorb energy and to deform in a specific way, this makes the automobiles frame into a complex system of different TWBs that need to work together in order to achieve the desired goals of stiffness, crashworthiness, and low weight.

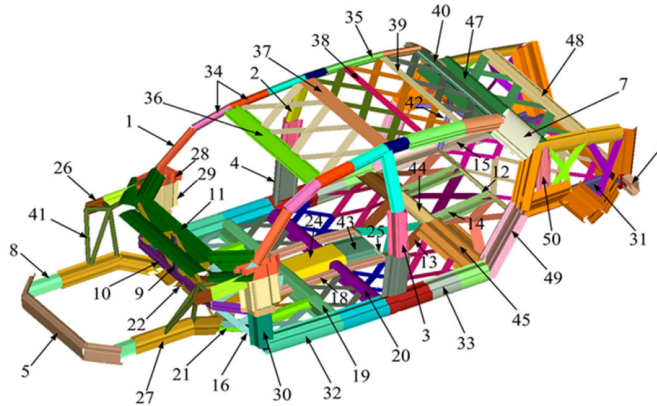


Figure 1: An example of a car frame, note the many different TWBs geometries [1]

Development of crash structures is time and resource-consuming because of the complexity

required verify the crash structures analytical, therefore finite element simulations are widely used. FEM is used to solve complex problems but requires substantial computing power to provide accurate results. In this thesis, the possibility to replace FEM (in an early stage) by predicting the behavior of thin-walled tubes when subjected to a dynamic axial load is researched. This prediction could be performed by analyzing the geometries before simulations are conducted, in order to see if any of the geometric parameter values can be used to foretell the results of the simulation. If possible to predict this behavior before FEM simulations are done a substantial amount of time and resources could be saved during the development process.

1.1 Iterative design process

An iterative design process is a simple concept that works by continuously improving a design. After a prototype is created it's tested to see whether it achieves its design goals. If the design doesn't achieve its design goals a new prototype is created and tested again, this process continues until the requirements are met. This process can not only be used for single components and parts but also for larger assemblies, therefore it is often used in product development[11].

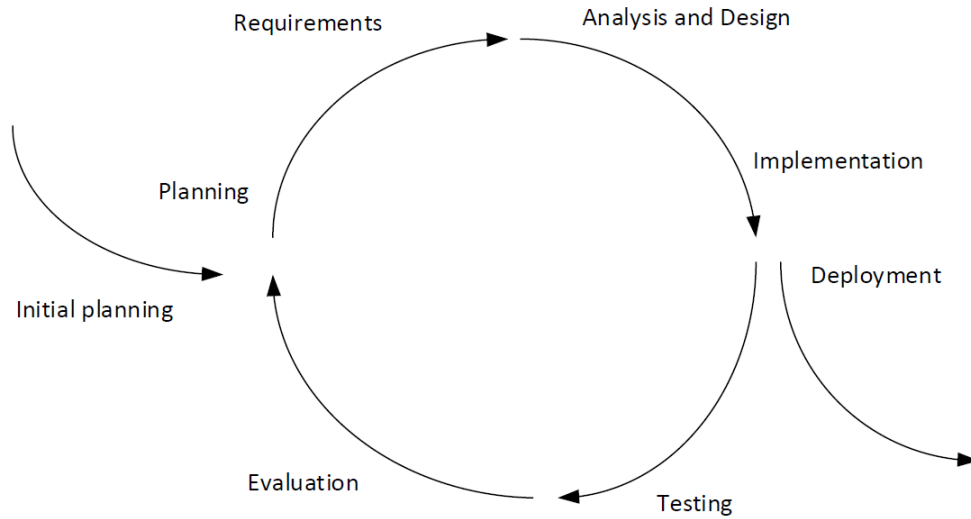


Figure 2: An example of an iterative design process.

When developing energy-absorbing thin-walled tubes an iterative design process is often used. This is because TWBs are designed to behave in a specific predefined way, in order achieve this many iterations are required where each iteration comes closer to the desired behavior. This way of development is resource and time-consuming since each iteration needs to be verified and simulated.

1.2 V-Model

A car is a complicated entity and to make it simpler to understand and design it is often divided into multiple subsystems. All subsystems and parts have special requirements that need to be fulfilled. An example of how the model works can be explained by using a car analogy. The requirements needed for the complete car can instead be divided into the appropriate subsystem. This makes it possible for a company to give different departments the possibility to work simultaneously on different systems or parts. This is also useful when doing FEM. Instead of analyzing the complete car, individual systems and parts can be studied before making the final assembly simulation. This approach is called the V-Model[2] is used in many industries and the car industry is no exception, the model is shown in figure 3. This model has been considered during the thesis and the reason why the beams have been studied individually and not in a system since if the beam fails the individual test it will not be used in the next stage.

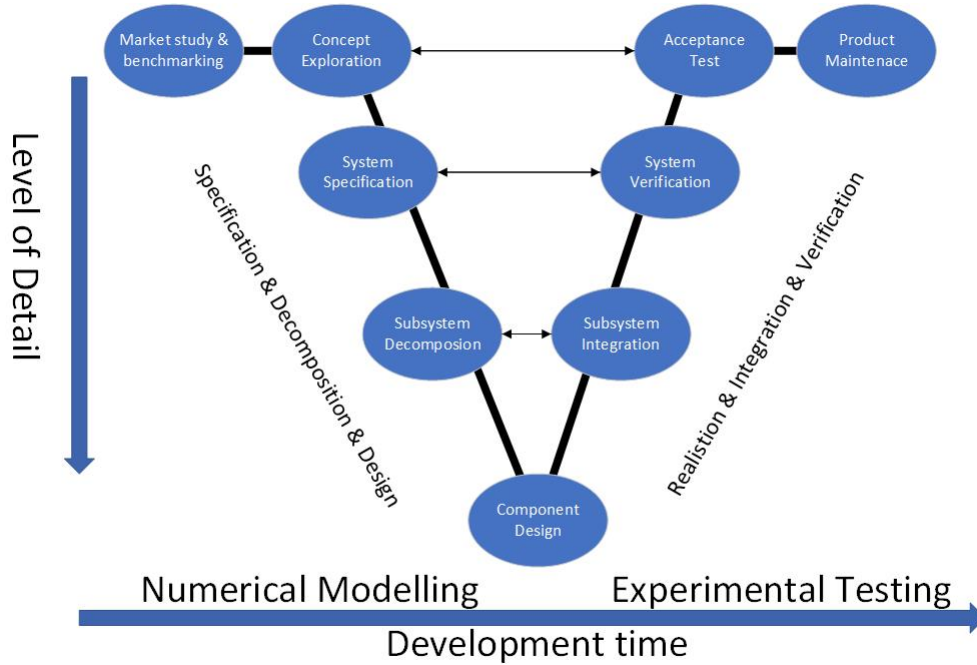


Figure 3: V-Model (Modified from source: Experimental Dynamic Substructuring: Analysis and design strategies for vehicle development [2])

1.3 Simulation driven design

In simulation driven design the choices made in the development stage are significantly supported by computer-based product modeling and simulation [12]. Simulations are used before a new system is build or an existing system is altered, in order to reduces the chances of unforeseen bottlenecks and to meet expectations while still being resource efficient. Utilizing simulation as a way to validate different systems necessitates trade-offs between simulation realism and simplicity [13]. Simulation driven design has the goal of shortening the

development process by analyzing the design from the very start of the development process. This makes it possible to verify different design choices quickly instead of needing to wait until the end of the development process but makes the designs very dependent on these simulations, this is also known as front loading [14].

1.4 Problem description

The iterative development process is often identified as a major cause of long product development lead times. A development lead time refers to the time it takes to design and verify a product, while the total lead time is the measured time from when a customer makes a request for a product until they receive it. Each iteration requires a considerable amount of manual CAE work and are a primary source of uncertainties when it comes to resource commitment. Product development lead time and cost reduction remain as a strategic priority for many organizations around the world.[14].

The automobile industry has over the last years moved away from physical testing and over to digital PD tools. This has shortened the total lead time but since automobile companies live in a highly competitive environment there is a constant need for improvement. In recent years a contributing factor to long lead times is the need to verify the performance of each iteration through simulations. Simulation models used in simulating crash scenarios involving automobiles are very complex, mainly because of the large amount of different parts involved in these simulations. Because of this in order to make the simulations accurate enough the simulations can last several days. These simulations are very demanding in terms of processing power and thus expensive for companies to conduct [15].

When designing TWBs and large TWBs systems such as the ones present in automobile frames many iterations are required leading to long lead times. TWB systems can be simplified [1] but this increases the error rate between the model and reality.

The main motive of this paper is to make the development process of thin walled tubes more efficient and cost effective which would in turn shorten the development lead times for TWBs. With improved lead times the development of TWBs becomes more cost efficient which in turn helps companies in a competitive marketplace.

1.5 Research question

This thesis aims to tackle this problem by trying to find a way to shorten the lead time for developing TWBs. By trying to find ways to predict how the TWB will perform before the verification process it might be possible to shorten the development lead time.

- What methods and tools are used today to shorten the development lead time for thin walled tubes?
- What are the main challenges in the development process for thin walled tubes?
- What types of methods can be developed to shorten the development lead time of thin walled tubes?

1.6 Delimitations

Because of time and resource restrictions, it was required to apply several limitations to the thesis. In the thesis only straight beams were analyzed. There were thoughts about having s-shaped beams and beams where the cross-section grows with its length. This required large modifications to the code and was not included in our research.

The amount of cross-sections geometries tested was also limited to 46, converting every cross-section into point coordinates was time-consuming, moreover the time needed for simulation, medial axis calculations and result gathering also increased with every cross-section.

The computing power used for the FEM simulations was limited, this contributed to long simulation times and required to use of smaller mesh size.

The verification of the FEM model was done by mimicking the results of a different research paper [16]. No physical test were done in order to verify the model, because of this errors in the mimicked paper could be transferred to our FEM model. Furthermore any error in the model would manifest itself in all the simulations and since the results are later compared to each other it would not impact the results.

Many of the geometries that are simulated have spot welds between the different plates see figure 4. To simplify the FEM process and since the welds are not of interest they have been neglected. When deciding to neglect the welds the report "Optimal crashworthiness design of a spot-welded thin-walled hat section"[17] was followed and it was found that the use of rigid-nodes was best suited for our application.

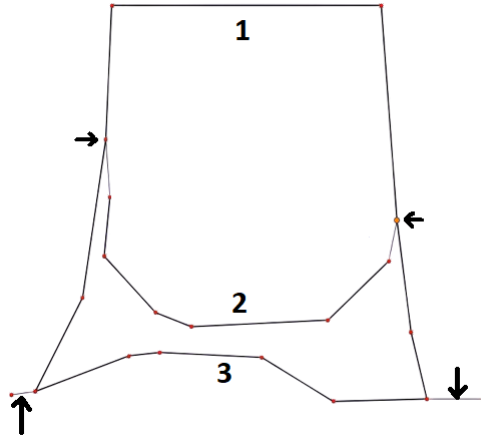


Figure 4: The figure visualizes three plates(Indicated by numbers 1, 2, and 3), and the arrows point at the welds between the plates.

1.7 Troubles during thesis

In order to automate Abaqus knowledge of the programming language python is required. Since this coding language was new to both of the authors a learning process was required. Furthermore, the Abaqus uses an old version of python 2.7.3(newest version 3.10.4 March 2022) which is not compatible with packages like numpy, xlswriter, or pandas packages. This created problems in the script that required workarounds. An example is the exporting of the results. Abaqus had problems when the script wanted to create and modify excel files. Abaqus simple export tool was the only thing that worked and another python based program was created to interpret and store the result in a file. When writing the code the macro function in Abaqus was often used. In some cases this led to problems, for example, we struggled for a while with selecting the surface on the analytical wall.

2 Literature review

Crash simulation is a key area in product design, especially in the automotive industry. In recent years FEM simulations have become paramount in the overall design process and not just in the verification step. Nevertheless, FEM analysis of crashworthiness is among the most complicated nonlinear problems in structural mechanics [18].

The challenge in developing TWBs is finding the optimal section configuration that satisfies all the crashworthiness requirements [3]. A typical design process for energy-absorbing structures can be seen in figure 5. First, the design space constraint is assessed, this impacts the geometrical shape of the energy absorbing structure. After this, the collapse mode is assessed this can be either local or global buckling. Finally, the mean crush force (MCF) and peak crush force (PCF) are calculated in order to see if the design reaches its performance requirements, this is often done with the help of FEM simulation.

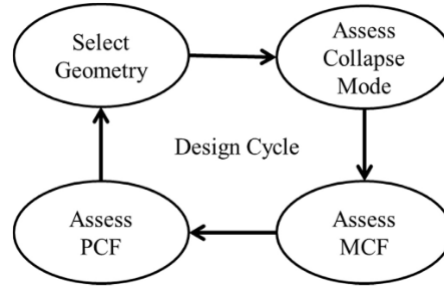


Figure 5: A typical design process for TWBs [3].

A typical use of simulation when developing energy-absorbing structures can be seen in the paper [19]. Here the authors investigate crashworthiness in collision events with s-shaped thin-walled rails/tubes of different shapes. Three main properties are researched, SEA(specific energy absorption), Fmax(Peak crash force), and CFE(crash force efficiency). The analysis is conducted with LS-DYNA and uses the explicit dynamic method. The models are created and imported from CATIA. To verify the analysis a real-life crash test is conducted on a squared thin-walled tube and later compared to the simulated results.[4]

Engineers often rely on their experience or repeat modifications to the cross-section design of TWBs in order to reach the desired mechanical properties. The paper [4] presents a method for optimizing TWBs cross-sections. The authors use a numerical genetic algorithm to achieve this. The goal of the algorithm is to minimize the total area (which represents the total weight of the beam) of the cross-section while maximizing the torsional rigidity and the moments of inertia. The geometries are modified by allowing the black points seen in figure 6 to move in the variable boundary (blue boxes). The authors conclude that this method is both efficient when it comes to processing power and effective in designing high stiffness and low weight TWBs.

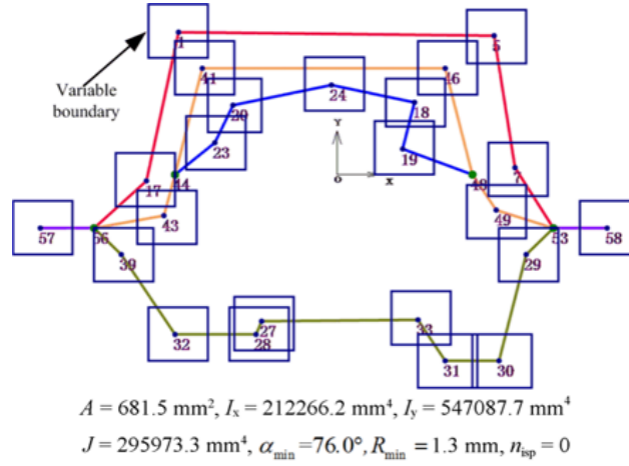


Figure 6: An example of a geometry before the optimization process is executed [4].

Since a big problem in developing TWBs is the long simulation time, effort has been put into shortening them. The paper [1] aims to accelerate the crashworthiness analysis of a vehicle structure. Instead of using detailed FEM models, they are simplified by using a plastic frame model which results in a simplified FEM model. The authors conclude that the simplified models deformation mode is basically the same and can be kept within a 5% error rate.

3 Theory

This chapter depicts the theoretical background for the thesis.

3.1 Thin walled tubes

Thin walled tubes are a popular way to achieve high crashworthiness while still being relatively cheap to produce. It can be very challenging for engineers to design the optimal thin walled tube since it requires trades-offs between strength, stiffness and energy absorption. Thin walled tubes absorb energy by buckling, this can occur in two main ways, global and local buckling. In global buckling, the structure's longitudinal axis is distorted or buckled while in local buckling the longitudinal axis is not distorted instead the length of the axis changes. Generally, local buckling is preferred due to much higher energy absorption capability. W.Abramowicz and N.Jones[5] showed that the way a tube buckles can be found by knowing the length and width ratio of a tube. They also show that the ratio can also be increased by increasing the width/thickness ratio.

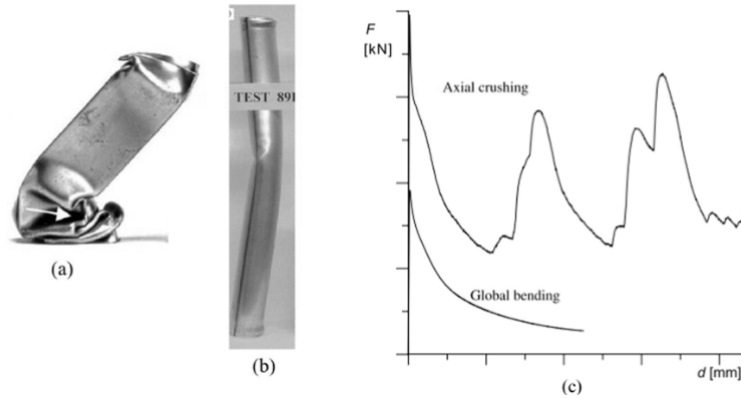


Figure 7: Example of global (b) and local buckling (a), in the corresponding load displacement graph (c)[5]

The use of different materials affects the energy absorption capability of thin walled tubes. Generally, metallic materials are used to manufacture TWBs, these materials generally absorb energy through progressive plastic deformation. Composite materials are also used[20], although these materials dissipate energy by fracture mechanisms. Composite materials can absorb more energy by weight but are more expensive to manufacture, they are also more difficult to simulate because of their anisotropic properties. Additionally, thin walled tubes energy absorption can further be enhanced by using filler material[6]. This filler material is generally made up of polymeric foams and metallic foams. Hollow thin-walled tubes can further be strengthened by utilizing multiple cell geometries[21].

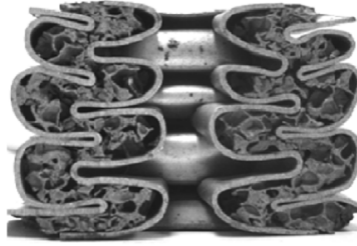


Figure 8: Thin walled tube with aluminum foam as filler material [6]

3.2 Energy absorption

When talking about energy absorption we refer to the area underneath the load-displacement graph. From this graph, we can evaluate several metrics used when assessing crashworthiness.

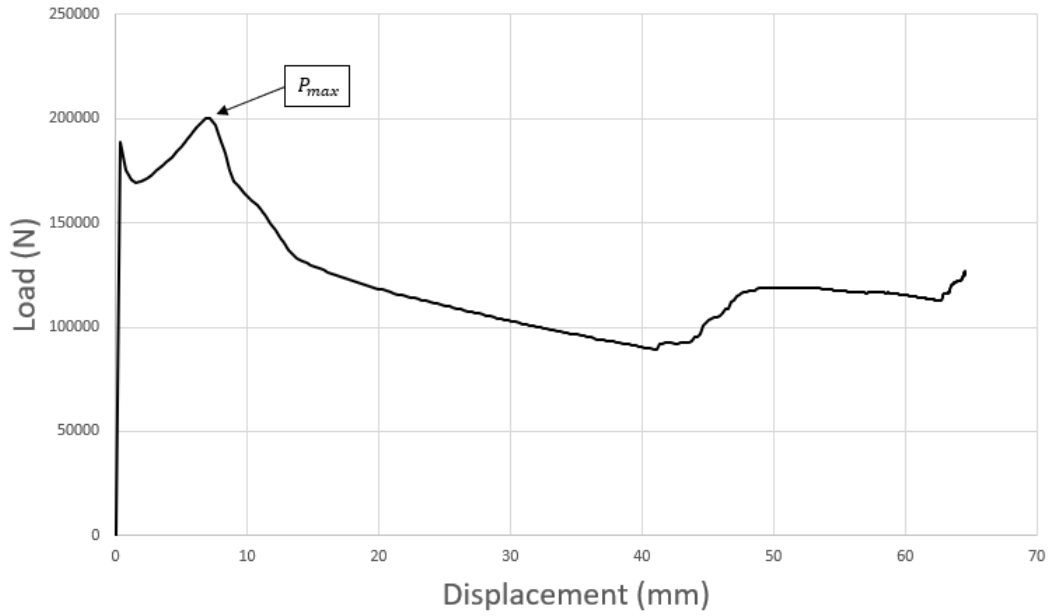


Figure 9: Example of a load-displacement graph

3.2.1 Peak crush force

The peak crush force P_{max} is defined as the maximum force reached in the load-displacement graph. This is one of the metrics that is used to later compare the results.

3.2.2 Total energy

The total energy [19] is measured in Joules (J) and can be found by calculating to total area underneath the load-displacement graph.

$$EA = \int_0^{\delta} P d\delta \quad (1)$$

3.2.3 Mean crush force

The mean crushing force[19] is calculated by dividing the total energy EA by the total deformation δ . This is used to verify the FEM model used in this thesis.

$$F_m = \frac{EA}{\delta} \quad (2)$$

3.2.4 Specific energy absorption

The specific energy absorption[19] (SEA) is described as the total energy divided by the total mass of the object. This metric is of great use when comparing different materials with each other, although in our thesis we will use it to compare different geometries.

$$SEA = \frac{EA}{m} \quad (3)$$

3.3 Energy absorptions in automobiles.

A heavy car needs more power than a light car to move forward and since a car frame stands for one-third of a car's total weight it is a high priority to lower the frame's weight.[22]. So to be able to get a safe car with low weight the common approach is to use thin-walled beams(TWBs). The TWBs have high strength and stiffness compared to their weight. There are three main categories for the TWB beams high strength and low stiffens, moderate strength and stiffness, and low strength and high stiffness. To get the different categories a ratio between width to thickness is used(b/t) [7].

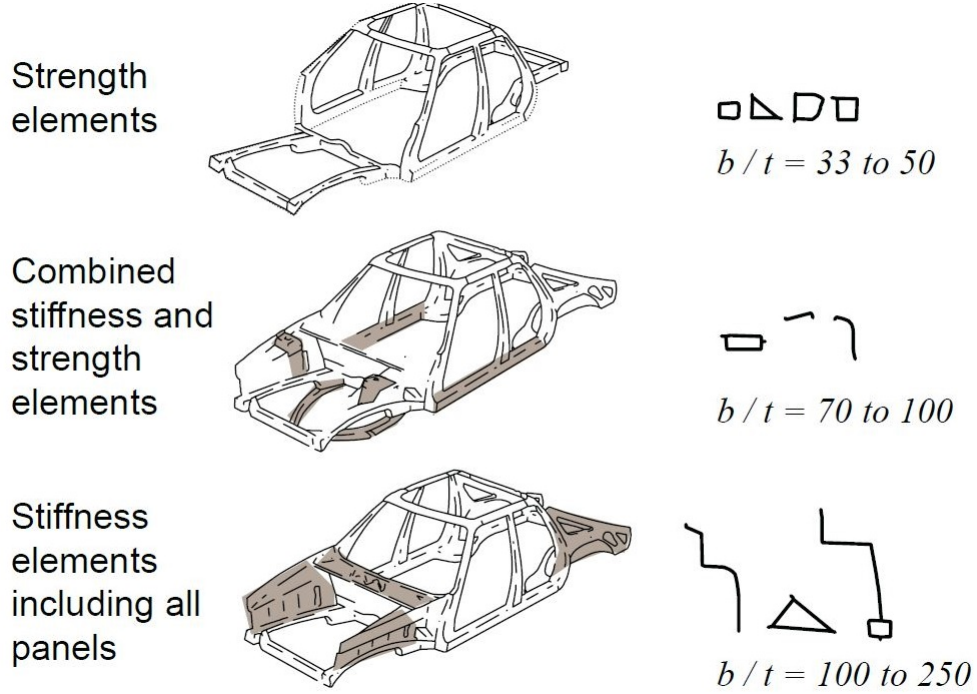


Figure 10: Stiffness compared to strength [7]

3.3.1 Unibody

In cars, there are two approaches to building the body of beams. The first way is a body on frame where the body and frame are built separately and when completed bolted together. The second choice is the unibody[23] which is one body that is welded together to form the framework of the car. In this thesis, the used geometries are taken from the article "Cross-sectional shape design of automobile structure considering rigidity and driver's field of view"[9] that studies unibody.

3.3.2 Materials

A car body consists of many beams and depending on their requirements and application there are various materials to choose from like mild steel, advanced high-strength steel, aluminum alloys, magnesium alloys, glass fiber reinforced plastic, and carbon fiber reinforced plastic [7]. Steel is mostly used but other lightweight materials like aluminum and magnesium alloys are used more and more in modern cars [24].

Much focus has in the later years been put on reducing the environmental impact of producing industries. One contributing factor is cars and their emission, to reduce to amount of emissions generated by cars the use of aluminium alloys[25] has started to replace steel. Aluminium weights less than steel which means less power is required to get the car in

motion, this equals less emission (steel is 2.5-3 times heavier than aluminium [26]). Nevertheless in order to achieve the same strength from aluminium as steel, a larger volume of aluminium is required.

3.4 Mesh

FEA uses CAD models to represent a physical model of an object. The mesh[27] [28] divides the CAD model into small parts called elements and they are directly related to the accuracy of the simulation results. The smaller the mesh the more accurate the simulations become but also more computer power and time is needed to find a solution for the simulation [29]. Inside the elements, polynomial equations calculate an approximation solution for the elements. When all the element solutions are combined they give an approximate result. The known values inside the elements are called nodes and are often located at the boundary of the element and connect the elements to each other.

3.5 Mass Scaling

Mass scaling [30] is a tool that can be used in FEA programs to save time in simulations. Mass scaling can be applied to individual elements or sets but also on the whole model. Mass scaling increases the mass of the selected elements which makes the stability limit higher. The stability limit determines the minimum size of the time increment that is needed for a simulation and the calculations supporting this can be seen in equation 4.

$$\Delta t_{stable} = \frac{2}{\omega_{max}}(\sqrt{1 + \xi^2} - \xi) \quad (4)$$

Where ξ is the fraction of critical damping, Δt_{stable} is the stability limit and ω_{max} is the highest frequency. This method takes the whole model into consideration and is based on a complex set of interaction factors. This makes the formula not computationally feasible to calculate, so instead, there is another formula that gives a close approximation, see equation 5 and 6.

$$\Delta t_{stable} = \frac{L^e}{C_d} \quad (5)$$

$$C_d = \frac{E}{\rho} \quad (6)$$

Where ρ is density, E is Young's modulus, L^e is element length and C_d is the wave speed of the material. This equation explains that stiffer material gives higher wave speeds and that results in a lower stability limit while a material that has a higher density is resulting in a higher stability limit. The stability limit is the amount of time needed for a dilatational wave across an element. This can be applied for example by setting a scale to target time increment of a value x and then by scaling if below minimum. This tells the elements with a stable time below the user specified time need to be mass scaled.

3.6 Python

Python is an interpreted, object-oriented, high-level programming language with dynamic semantics [31]. This language is compatible with Abaqus script and is therefore used in the automation of Abaqus. Before this thesis work, the language were not known to the participants. To learn the language Python tutorials and Abaqus macros were used. Macros record changes in Abaqus, these macros are then shown in code to the user, see chapter 4.3 for more information about macros.

3.7 Automation

Automating different processes is a common implementation in the world of engineering, three reasons for this are that automation saves time, ensures quality, and saves money. When deciding if a company should implement an automation process the company needs to understand if the process is possible to automate and how much money it could save them. These two factors need to be considered since automating is often costly. The more standardized a company's processes are the easier they are to automatize, while in companies that have more unique processes and components it can be harder.

When making CAD models and FEM simulations the time needed to create them can be long, so they are often automated when possible. One common approach for this is to parameterize the CAD model, see chapter 3.8. Parameterized models can be modified quickly by only changing the values of the parameters.

In this thesis, one of the focuses has been to automate the design and analysis. In our thesis, the models look very different from each other and the possibility to create one parameterized model and modify it for all cross-sections was not possible. Instead, the process was automated and the cross-sections were stored and retrieved from a database.

3.8 Parametrization

When designing shapes for different design goals parameterization is often used. When the dimension of a parameter in a parametric model is changed the modeling process can change the shape of the model automatically. Parametric models are often used in CAD modeling, this method eliminates the need to redraw the model every time a parameter is changed.

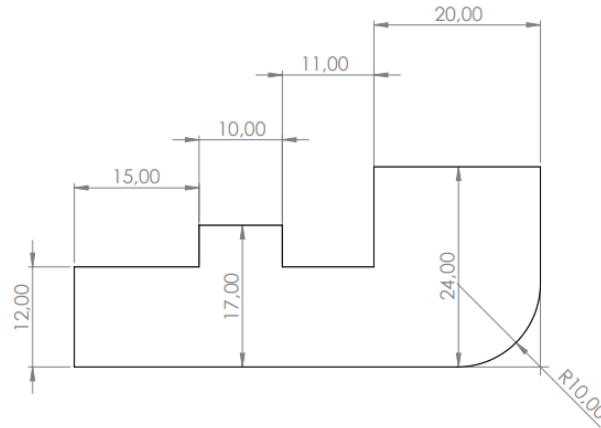


Figure 11: Example of a parameterized 2d geometry

3.9 Medial Axis

The medial axis is defined as following: a given object represented by an polygon curve C , the medial axis $M(C)$ is a collection of points p inside C that have at least two points on the boundary C with equal distance and are closest to p [32].

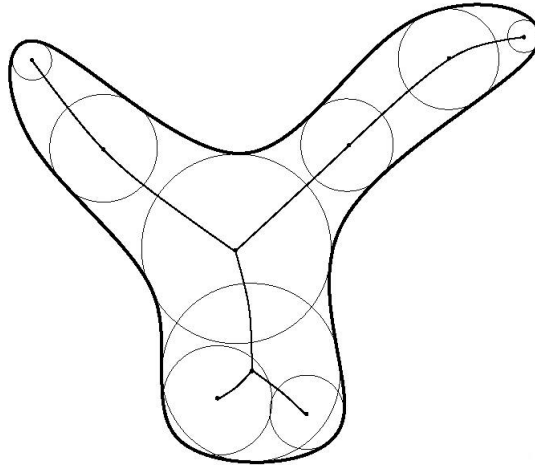


Figure 12: Example of a geometry with a medial axis [8],

4 Methodology

4.1 Cross-section geometries

The cross-section geometries for the beams used in the thesis are taken from another scientific paper[9], see figure 13. In their work they optimize an A-pillar of a Toyota RAV4 considering the drivers field of view and the rigidity of the beam.

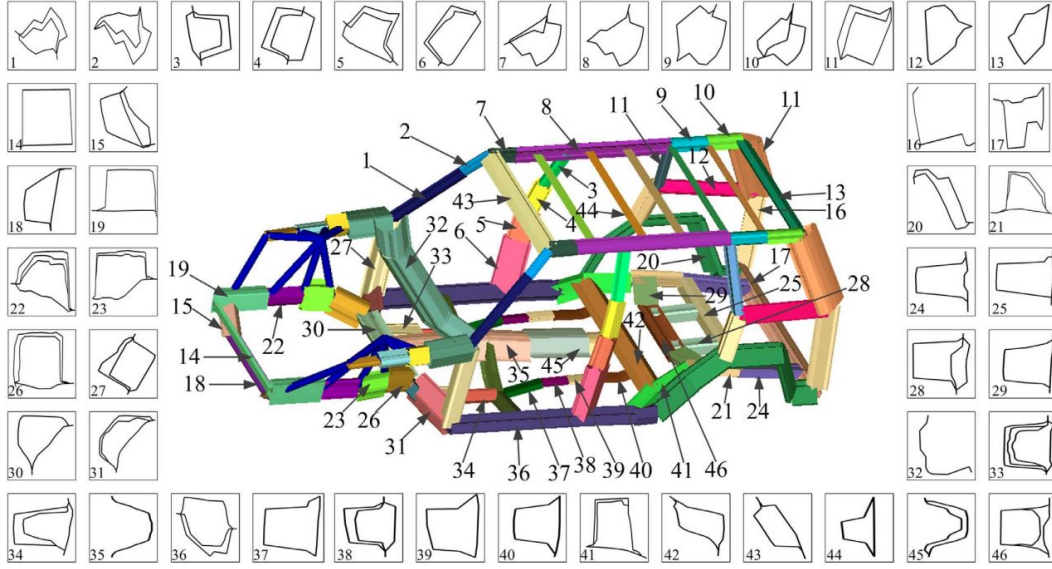


Figure 13: Car frame with beams [9].

The geometries are a simplified representation of a Toyota RAV4's frame. Since no other information than the images of the geometries was given the first task was to find a way to represent the geometries. To get a similar scale on the beams the complete image with all the beams was imported into SolidWorks. Then points were placed on the geometries where a change occurred, and the x and y coordinates were recorded in Excel. When all the cross-sections are in one image the cross-sections get one global coordinate system. For example, in cross-section 46 the starting coordinates are 1184,-291. This is a problem since it means that when Abaqus will build the cross-section it will not start in the middle 0.0, and 0.0 and can be so far away that the wall and beam won't collide. To avoid this the first point in each cross-section was subtracted from itself and all other points in the cross-section creating a local coordinate system. This process can be viewed in 2 and in 14. In this specific case that is shown, there are two edges that are only connected on one side. That is indicated by the numbers 5,5 and 10,5 which means that the line is connected with 5 and 10 respectively but nothing on the other end. All of the points were used in a text document that Abaqus read to create the beams.

Original			Translate		
Outer Shape	x	y	Outer Shape	x	y
1	1184,273	-291,225	1	0	0
2	1184,273	-238,233	2	0	52,992
3	1226,503	-235,135	3	42,23	56,09
4	1248,516	-232,363	4	64,243	58,862
5	1261,56	-229,2655	5	77,287	61,9595
6	1262,049	-247,69	6	77,776	43,535
7	1253,407	-261,713	7	69,134	29,512
8	1252,429	-281,768	8	68,156	9,457
9	1253,08	-287,8016	9	68,807	3,4234
10	1260,09	-306,22	10	75,817	-14,995
11	1241,667	-296,932	11	57,394	-5,707
12	1210,524	-292,367	12	26,251	-1,142
Inner Shape	x	y	Inner Shape	x	y
12	1210,524	-292,367	12	26,251	-1,142
13	1221,938	-291,55	13	37,665	-0,325
14	1233,515	-292,693	14	49,242	-1,468
15	1244,602	-282,583	15	60,329	8,642
16	1247,37	-275,572	16	63,097	15,653
17	1246,07	-248,668	17	61,797	42,557
18	1234,493	-236,765	18	50,22	54,46
3	1226,503	-235,135	3	42,23	56,09
Edge1	x	y	Edge1	x	y
5	1261,56	-229,2655	5	77,287	61,9595
5,5	1261,56	-218,01	5,5	77,287	73,215
Edge2	x	y	Edge2	x	y
10	1260,09	-306,22	10	75,817	-14,995
10,5	1260,745	-310,955	10,5	76,472	-19,73

Table 2: Beams 46 coordinates recorded in sheet based on the figure 14.

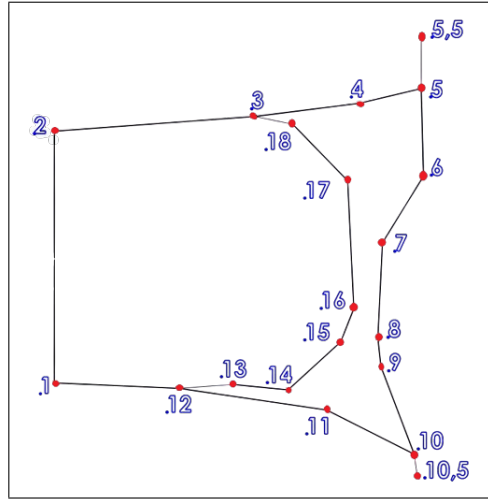


Figure 14: Beams 46 coordinates in the order that they have been recorded, see the table 2.

4.2 Studied case

In this chapter the setup used in the finite element simulation will be displayed.

The finite element simulation performed in this case has been conducted in Abaqus. The simulation is a dynamic explicit simulation and is a simulation of a collision between a thin-walled tube and a rigid wall. The beam is locked in place while the wall moves towards the beam crushing it in an axial direction. To make the simulation realistic different mesh sizes were tested and material properties for the used material were researched. The complete setup can be read throughout this chapter.

Each cross-section geometry was extruded 100mm resulting in a 3d shell part.

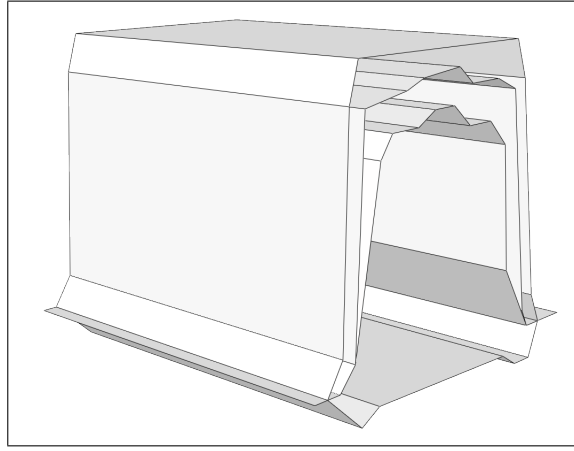


Figure 15: Picture of extrude geometry 33.

All the geometries were tested for 3 different thicknesses, since increasing the thickness increases the energy absorption capability of the tubes the mass of the is also increased.

Thickness (mm)	Wall mass (kg)	Wall velocity (m/s)	Wall Kinetic Energy (J)
1	50	8	1600
2	100	8	3200
3	250	8	8000

Table 3: Analytical wall properties

The mass and velocity of the wall analytical that impacts the tube was chosen by doing multiple test simulations, it was important to achieve a plastic deformation of the tubes while not having too much kinetic energy in the wall so to deform the tube to a level where the wall impacts the boundary fixed locations at the end of the tube, this was accomplished by checking each simulation manually. A dynamic explicit simulation step is used for the simulations. Mass scaling is used to decrease the simulation time. In this study, a semi-automatic mass scaling was used on the whole model. Multiple tests were done in order to

find the most suitable time target increment, in our case this was $5e-7$. In order to stop the simulation at the correct time a filter is used, this filter monitors the speed of the analytical wall and stops the simulation when the wall velocity reaches 0. This way of stopping the simulation might result in a small error since it does not allow the tube to spring back. A penalty friction coefficient of 0.45 was used to describe the interaction between the tube and wall. The analytical wall is locked for all movement except for one axis, the Z-axis. The tubes were locked in place at the endpoint nodes, the type of boundary condition for the tube is encastre which locks it for all degrees of freedom.

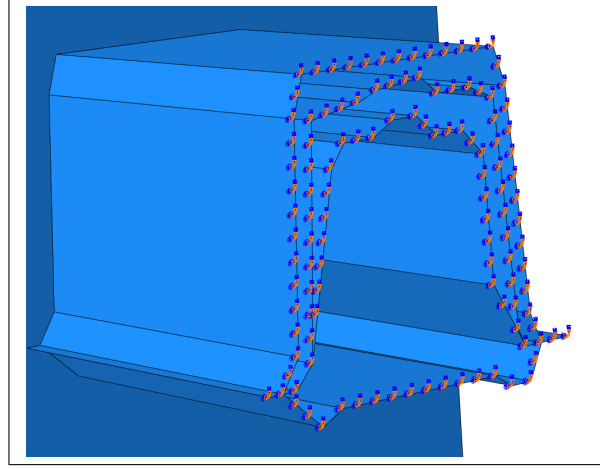


Figure 16: Picture of the boundary condition applied to geometry 33.

From the FEM validation, we noticed that the most accurate results were found with a mesh size of 1,5mm. Unfortunately, it was noted that using this mesh size for all our simulations was not possible, the simulation would often crash or take hours to complete, so instead, a 2mm mesh size was used. This mesh size is not as accurate of reality as 1,5mm but since we are comparing the results from the FEM simulation with each other this won't impact the results.

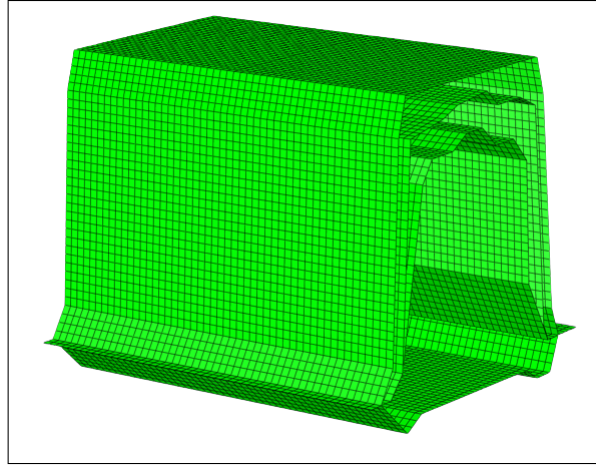


Figure 17: A picture of a fished mesh, geometry 33.

Several output variables are requested from the simulation, all these variables are requested every $5e-5$ seconds of the simulation. The reaction force is the first variable requested, this is measured at every node in the tube's boundary condition. The other two variables are the velocity of the wall displacement, since the wall touches the tube at the beginning of the simulation the measured amount of wall displacement is the same amount the tube displaces.

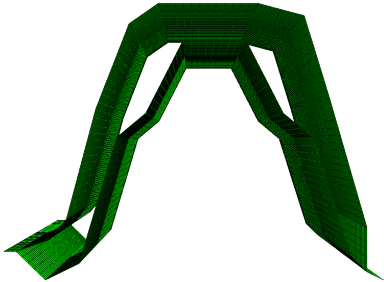
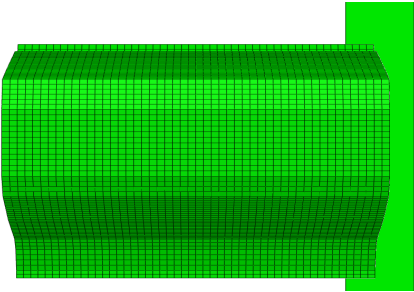
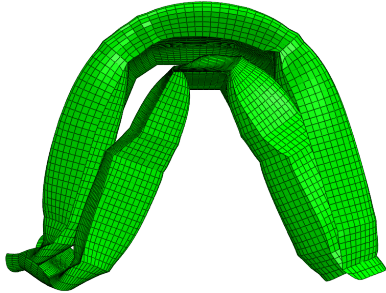
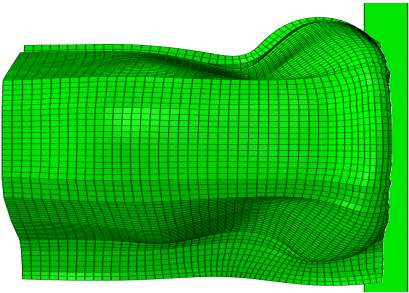
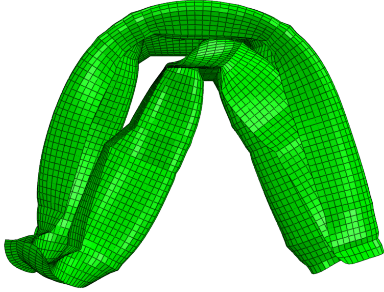
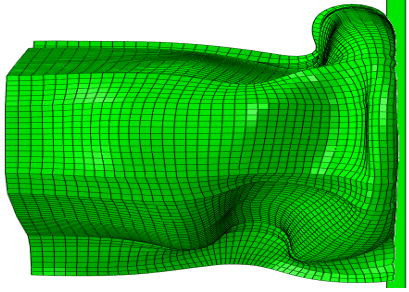
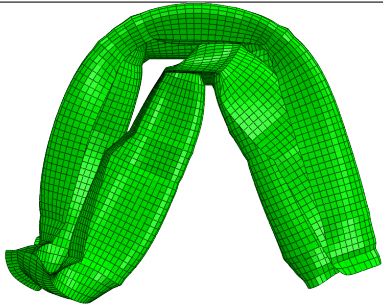
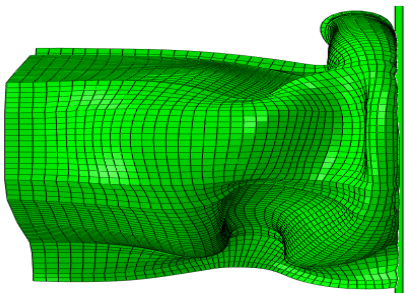
Time Step (%)	Front View	Top View
0		
33		
66		
100		

Table 4: An example of a geometry 45 being crushed with 4 different time steps, the beam is seen from the front and top.

4.3 Finite element automation

To be able to use the script in Abaqus the first thing the code does is to import modules. These modules are necessary for the program to work and tell the program how to interpret the code [33]. After that, the script imports functions that were created by the author but stored in a different file to make the code more structured. The next step in the code is to insert information about variables that the code uses, these can easily be changed for example Length of the beam and thickness see table 5.

Variable	Name/Value
Model	Sets the model name
Part	Sets the name of the part
Step1	Step1 is "Initial" since it is the preset name for step one and it is not changed
Step2	Sets the name of the second step
Length	Sets the length of the beam
Thickness	Sets the thickness of the beam
BeamSection	Sets the name for the section
Material	Sets the name for the material
Database	Put the name of the database file
MassScalingFactor	Sets the mass scaling for the mesh
WallMass	Sets the mass for the wall
WallVelocity	Sets the velocity for the wall
FrictionCoefficient	Sets the friction coefficient
MeshSize	Sets the mesh size for the beam
Time.Period	Sets the time for the simulation
Wall.Height	Sets the wall height
Wall.Length	Sets the wall length
Wall.To.Beam.Distance	Sets the distance between the wall and beam
History.Time.Interval	Sets the time interval for the history output
Section.Offset	Sets the section offset
Result.Location	Sets the saving file location for the results
NumbersDomains	Sets the numbers of domains the simulation can use
NumbersCpus	Sets the numbers of CPU's the simulation can use
Density	Sets the density for the material
Elastic	Sets the Young's Modulus and Poisson's Ratio
Plastic	Sets the Yield Stress and Plastic Strain

Table 5: Variables

The last thing before the code starts to create things in Abaqus is to import information about the cross-sections from database.txt. Now the loop that creates all the simulations starts, the functions beneath are all the functions used in the program to create one beam.

- Create_Material function creates material in Abaqus. The variables that the user can change are Name, Density, Elastic, and Plastic. When these parameters are set the program can create the new material.
- Create_Step creates a new dynamic explicit step for the simulation. The simulation needs to know the previous step to know when it should be activated. Other variables that the function has are mass scaling factor, time period (the length of the step),

name of the step, and a description of the step.

- `Create_Section` selects a given part and applies a homogeneous shell section. The variables that can be changed in this function are which material should be applied and the thickness of the section.
- `Create_Mesh_Part` creates a mesh on the given part. The variable change that the user can do in this function is to change the mesh size.
- `Create_Friction` creates an interaction between different parts/objects in a specific step. The Interaction will be contact and have the Mechanical property/tangential behavior/penalty and the friction coefficient can be changed by the user.
- `Create_Node_set_ByBoundingBox` creates a node-set. By entering six coordinates x_1 , y_1 , z_1 , x_2 , y_2 , and z_2 the function creates a three-dimension box in space and all nodes inside the box become a set for a specific part.
- `Add_Part_To_Assembly` adds a specified instance of a part to the assembly.
- `Fix_nodes` is a BC (boundary condition) of type symmetry/Antisymmetry/Encastre. The user can decide in which step it should be activated and on which node-set, the BC locks all degrees of freedom ($U_1=U_2=U_3=UR_1=UR_2=UR_3=0$). The degrees of freedom [34] represent displacement in x , y , and z plus rotation in x , y , z .
- `Create_Element_Set_ByboundingBox` creates an element set. By entering six coordinates x_1 , y_1 , z_1 , x_2 , y_2 , and z_2 the function creates a three-dimension box in space and all elements inside the box become a set for a specific part.
- `Build_Wall` is a function that got its own file to give it a clearer structure. The function creates an analytic rigid surface 4.3 that is used to deform the beams in the simulations. The parameters that the user can define are length, height, mass, distance between beam and wall, and velocity of beam.
- `Create_Simulation` creates and submits the simulation in Abaqus, the user can select numbers of domains 4.3 and coarse that should be used.
- `Create_part_from_txt` takes the coordinates from the txt file and creates the cross-section, it also takes the information about how long the beam should be when finished.

Macros or macroinstructions is a tool that records actions performed in a program for example Abaqus. When the recording is stopped the performed actions will be translated

to code that the user can view. For example, in this macro, a feature called Beam1_Instance that is a part of the model CrashSimulationModel was deleted, this gave the following macro.

1. a = mdb.models['CrashSimulationModel'].rootAssembly
2. del a.features['Beam1_Instance']

This is how the program understands the performed action in code and this can now be used and modified by the user to delete other features and if the user needs to do another action a new macro can be recorded.

The database (txt file) information was entered manually by the authors and is semi-automated. The file contains information about the total numbers of geometries, numbers of coordinates, and the coordinates themselves.

The analytic surface [35], also known as rigid wall, is created by defining 2-dimensional cross-sections along the global x, and y axes and is extruded along the z-axis. The motion and the degrees of freedom for the surface are controlled by the reference node/point. This type of body where one node controls a compilation of elements, surfaces and/or nodes is called rigid body [36]. The shape and position of the elements and/or nodes are constant during a simulation and can not deform. But the whole model can be moved by adding motion to the reference node.

Domain-level parallelization or Domain divides the analytic process into parts that can be done in parallel to each other. The domains [37] divide the model into the specified number of topological domains. These domains are evenly divided between the available processors and can process the individual analysis parallel to each other. But since the domains share common boundaries, they need to send information between each other in every increment.

The results exported from Abaqus are stored in Excel CSV files. Abaqus exports and stores one file for each result and simulation, this created two files for each simulation. So, another Python program was created that transforms the CSV files to xlsx files, then it takes out SEA and Max force from the xlsx files and creates a new combined file with all the simulations and results. When the combined file is created the program deletes the remaining files.

The final step of the code is to gather the peak crush force and calculate the SEA. The peak crush force is calculated by summing all the forces in the longitudinal direction in the fixed nodes.

4.4 Feature extraction

In our thesis 46 different cross-sections are to be parameterized in such a way that makes it possible for them to be compared to one another. This requires parameters that all cross-sections share. Three types of parameters that all geometries share are: circumference, medial axis length, and area. Furthermore, the ratio between the circumference and medial axis length is also used.

4.4.1 Rhino Grasshopper

All the different parameters were calculated with the help of Rhino Grasshopper. Rhino is a 3D design software used for industrial design. Grasshopper is a plug-in to Rhino and is a modeling tool that utilizes visual programming to design complex geometrical shapes with the help of certain parameters. The geometries different points which represent the different corners and angles in the cross-section were written into a large Excel file. Rhino grasshopper later imports the coordinates for every point from the excel file and constructs lines between them. From the constructed geometries the different parameters are calculated. A visual representation of the Rhino Grasshopper code can be seen in the figure 18:

- Blue portion: In this part of the code the geometry is imported from the excel file, this is done by first selecting which geometry is to be imported, the code then sends the coordinates for each point to the red portion of the code.
- Red portion: Here the code constructs the geometries with the medial axis from the coordinates sent to it. The code also calculates the values for each parameter of the selected geometry, these parameter values are later sent to the green portion of the code
- Green portion: The green portion of the code receives the values for the 4 different parameters (Circumference, area, medial axis length and M/C ratio). These 4 values are then saved in the excel file.

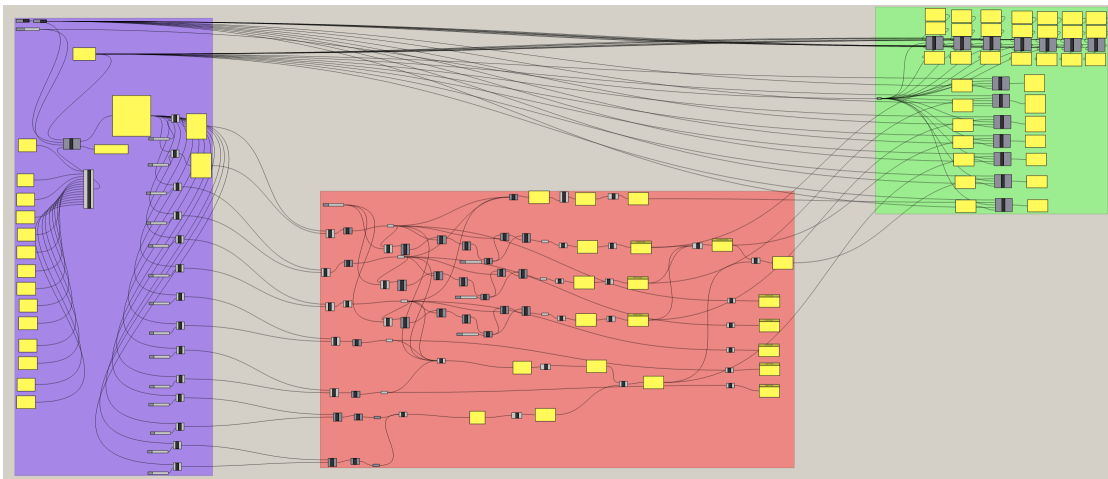


Figure 18: The visual representation of the Rhino grasshopper code.

4.4.2 Circumference

The circumference of the geometries was calculated with Rhino Grasshopper is represented in the figure 19 in black.

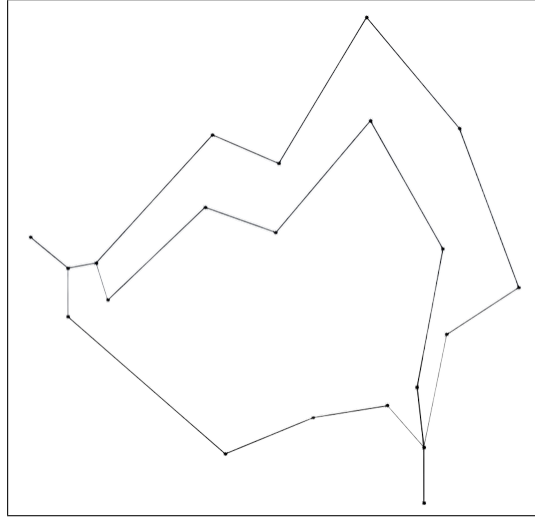


Figure 19: Geometry with circumference (black)

4.4.3 Area

The Area of the geometry is also calculated in Rhino, the area of the geometry is the total area of the cross-section, ignoring the number of cells. An example of a calculated area can be seen in figure 20.

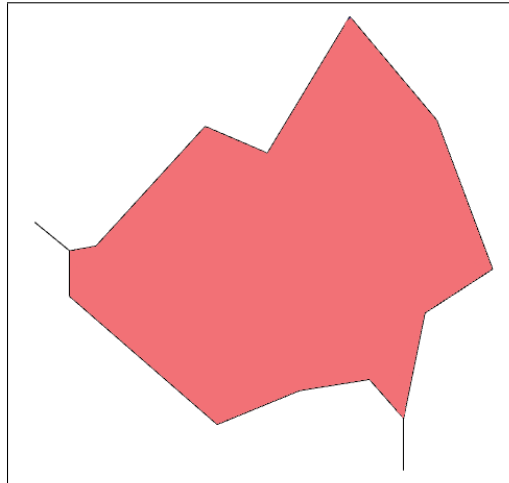


Figure 20: Total area of the geometry

4.4.4 Medial Axis

In this portion, it's shown how the medial axis is calculated in Rhino Grasshopper. The point coordinates are imported from the excel file and placed on a plane, after this the lines between the points are constructed as shown in the figure 21.

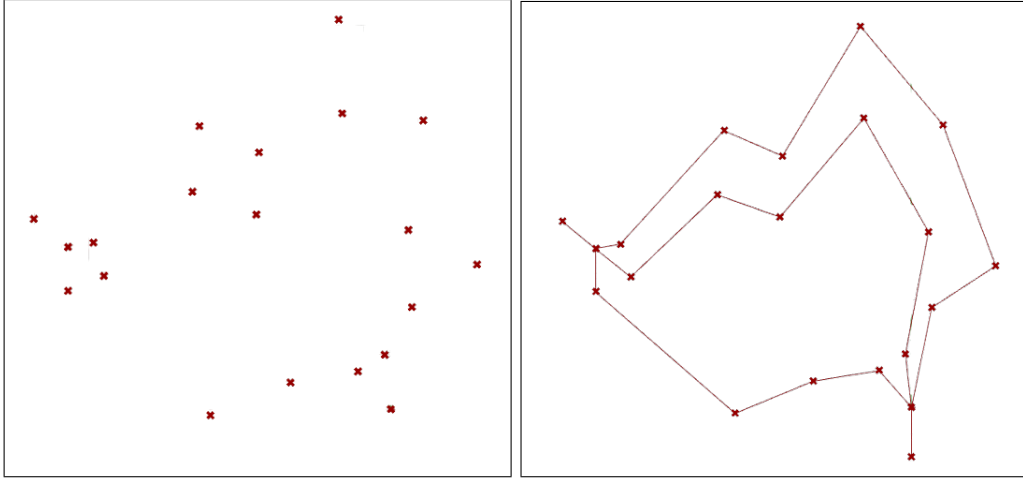


Figure 21: The imported points in Rhino, The constructed lines from the imported points in Rhino.

After the lines have been created the medial axis is constructed. This is done by dividing the circumference into multiple points.

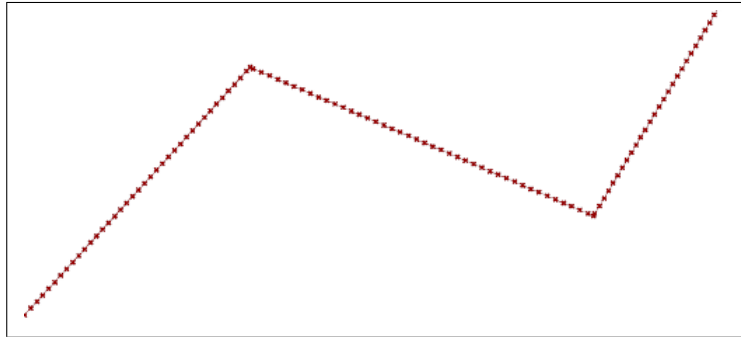


Figure 22: The circumference divided into multiple points

With the circumference made up of multiple points, a Voronoi diagram operation is executed. Here every point in the circumference acts as a seed for the Voronoi cell.

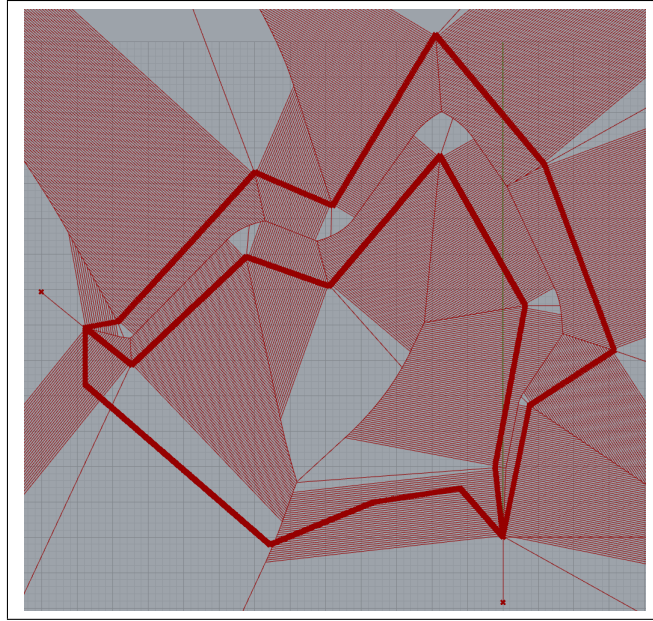


Figure 23: The geometry after the Voronoi operation.

The geometry was later cleaned by removing all the lines except the medial axis. The remaining geometry can be seen in figure 24.

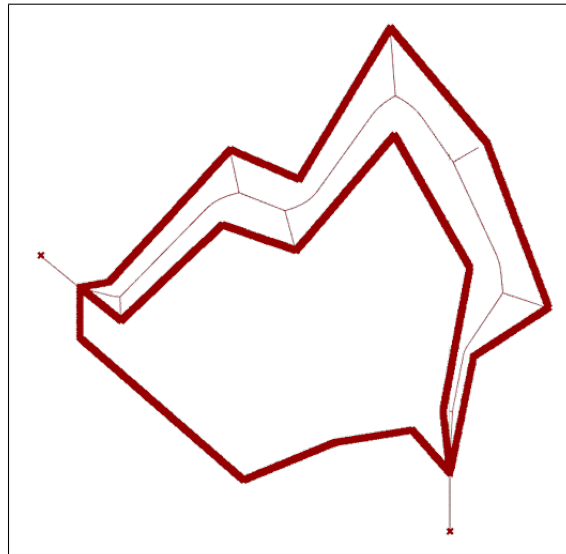


Figure 24: Cleaned geometry showing the medial line in one of the cells

The operation is later conducted for each cell in the geometry.

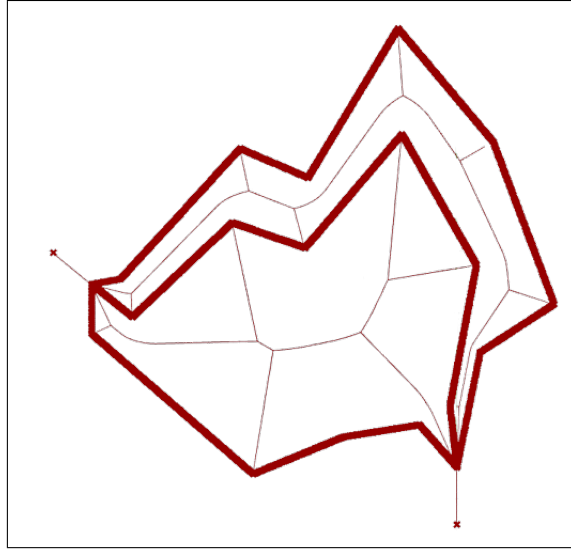


Figure 25: The geometry after the second medial line has been calculated

4.4.5 M/C ratio

The final parameter chosen to be investigated is the medial axis length divided by circumference ratio. This ratio shows how long the medial axis is compared to the circumference.

4.5 Verification data

In order to verify that the results correspond accurately to real-world situations, a comparison of the finite element model was conducted. During the thesis work, we didn't have access to material testing equipment therefore the material model was validated with the help of the paper written by D. Al Galic and A. Limam[16]. In the paper, the authors conduct quasi-static and dynamic tests on cylindrical tubes made from A6060 T5.

4.5.1 Material Model

The material data was acquired from the referred paper and is shown in table 6:

Density	2.7g/cm3
E Modulus	69.5 Gpa
Poisson Ration	0.33

Table 6: Material Data

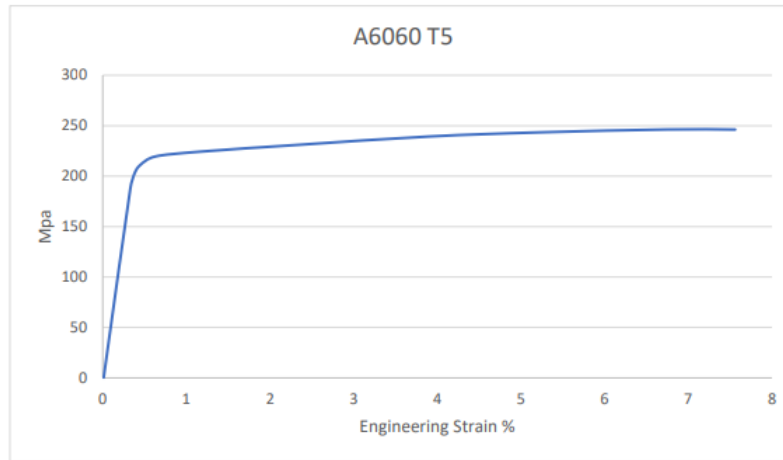


Figure 26: A6060 T5 Engineering Strain

4.5.2 Verified Geometry

The geometry used in the experiments consists of a 200mm long tube with a diameter of 60mm and a thickness of 2mm.

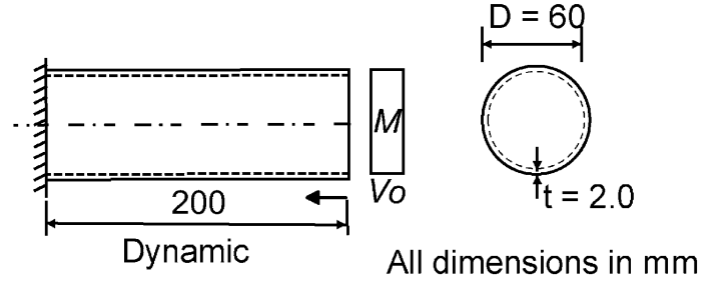


Figure 27: Test specimen geometry [5]

4.5.3 Test rig arrangement

The test rig in the experimental tests used in the referred paper[16] is composed of a truck on rails with an additional carrying truck on top, this top truck carries the desired weight and a solid wall that makes contact with the tube specimen. The tube specimen is mounted on a fixed plate, behind this plate sit the displacement cell and load sensor. A speed sensor is mounted under the carrying truck.

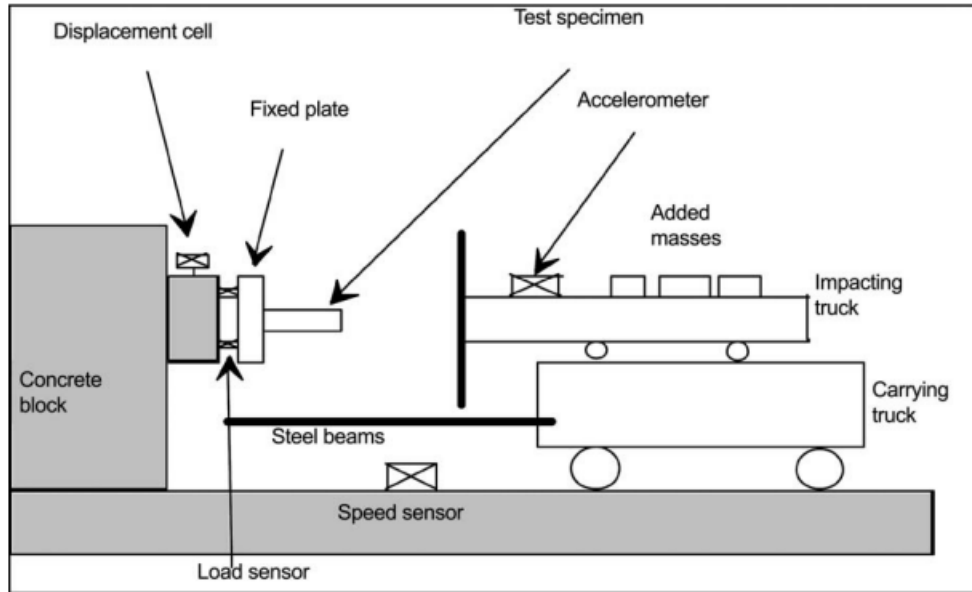


Figure 28: Test rig arrangement [5]

In the paper six different dynamic tests were done, these specimen are called (DRA01, DRA02, DRA03, DRA04, DRA10, DRA11). From these tests two were selected to be compared and validated to our model (DRA03 and DRA11). The tubes used in these tests are same geometrically, what differs is the mass and velocity of the impacting wall as can be seen in the table 7.

Test no.	Velocity (m/s)	Mass (kg)
1 (DRA03)	7.2	87
2 (DRA11)	7.83	117

Table 7: Experimental test data

The three different metrics recorded from the physical test are P_{max} , F_m and δ , these metrics are later compared to the values from the FEM model.

Test no.	$P_{max}(kN)$	$F_m(kN)$	$\delta(mm)$
1 (DRA03)	106	38	53
2 (DRA11)	120	38	85

Table 8: Experimental test results

4.5.4 Mesh convergence study

A mesh convergence study was done in order to choose the optimal mesh size. Mesh size was compared to the peak crush force, mean force, displacement, and simulation time. These tests were done on test no. 2 (DRA11) and later further validated by using the same settings for test no. 1 (DRA03).

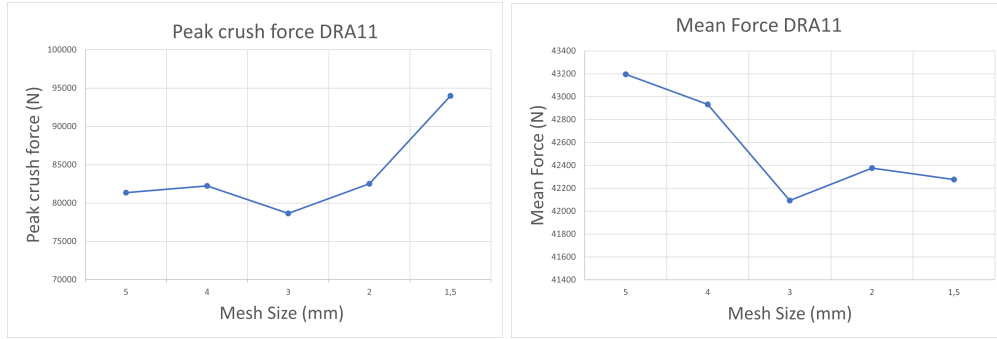


Figure 29: Peak and mean crush force compared to mesh size

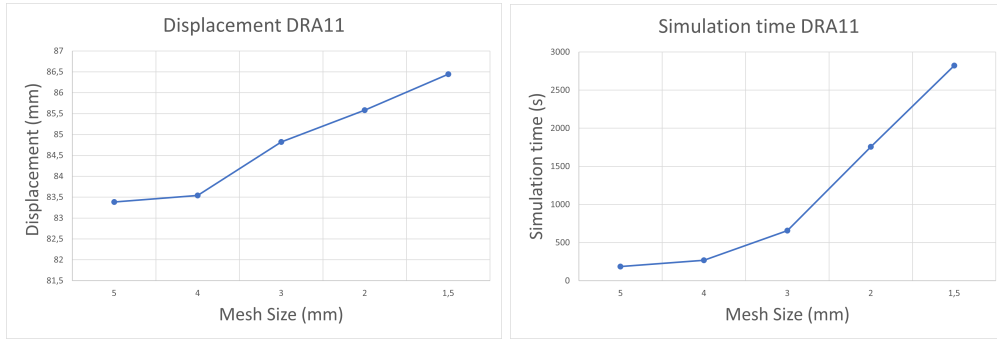


Figure 30: Total displacement and simulation time compared to mesh size

4.5.5 FEM validation results

The results from the FEM simulations are shown in the table 9.

Test no.	$P_{max}(kN)$	$F_m(kN)$	$\delta(mm)$
1 (DRA03)	93,2	42,3	53,2
2 (DRA11)	94	42,3	86,4

Table 9: FEM validation results

The error rate show how much the simulated results differ from the physical ones. These error rates can be seen in the table 10.

Test no.	$P_{max}(kN)$	$F_m(kN)$	$\delta(mm)$
1 (DRA03)	13,7%	11,3%	0,3%
2 (DRA11)	21,68%	10,12%	1,7%

Table 10: FEM validation error rates



Figure 31: Experimental result of DRA11 compared to the simulated result

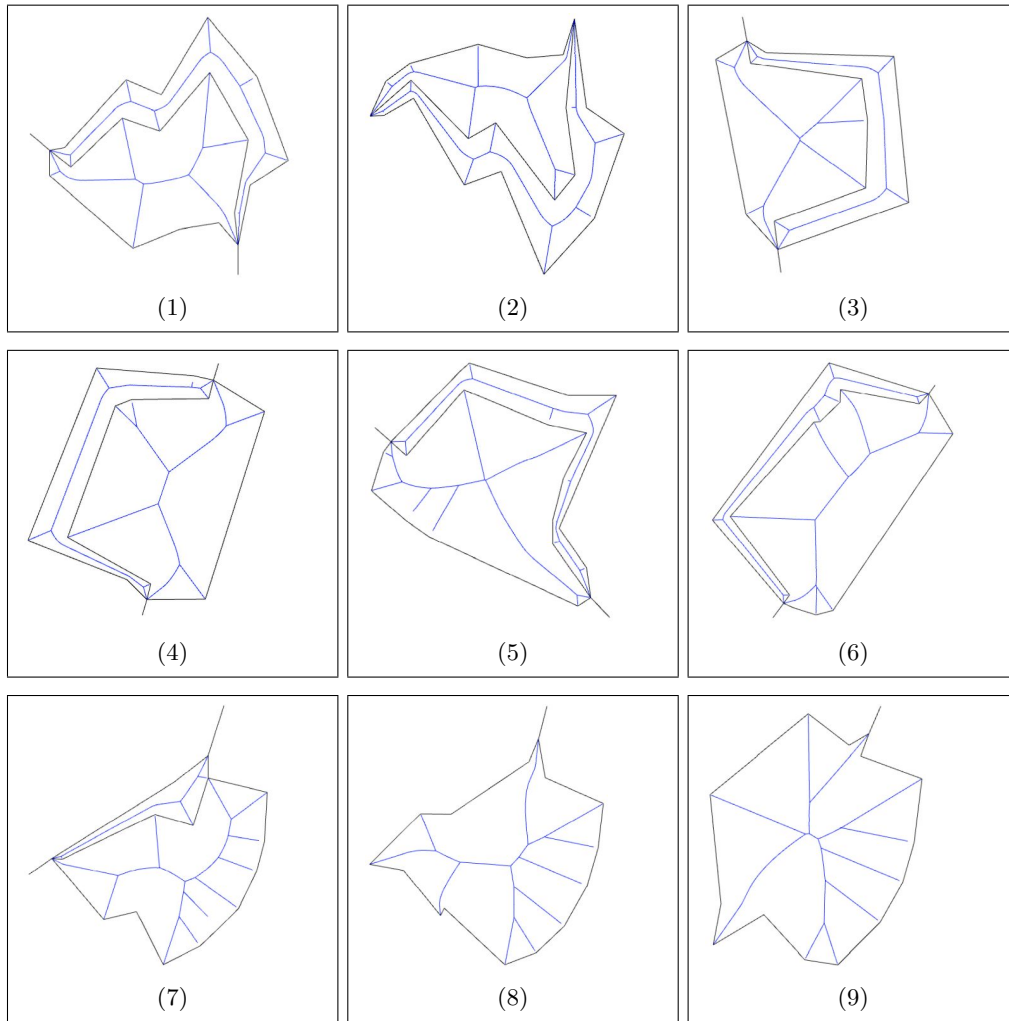
The mesh convergence study shows that as the mesh size is decreased the results better relate to the experimental results, although the simulation time increases severally between each step. From the graph, we can gather that none of the graphs have converged a satisfactory amount, unfortunately, due to limitations in processing power we were unable to successfully decrease the mesh size under 1,5mm, after this the simulation times increased dramatically. From table 10 it's noted that the biggest discrepancy between the experimental and simulated results is found in the peak crushing force and the mean crushing force, the error rate in the displacement is much lower with 0,3% and 1,7%. Nevertheless from these results the FEM model is considered validated.

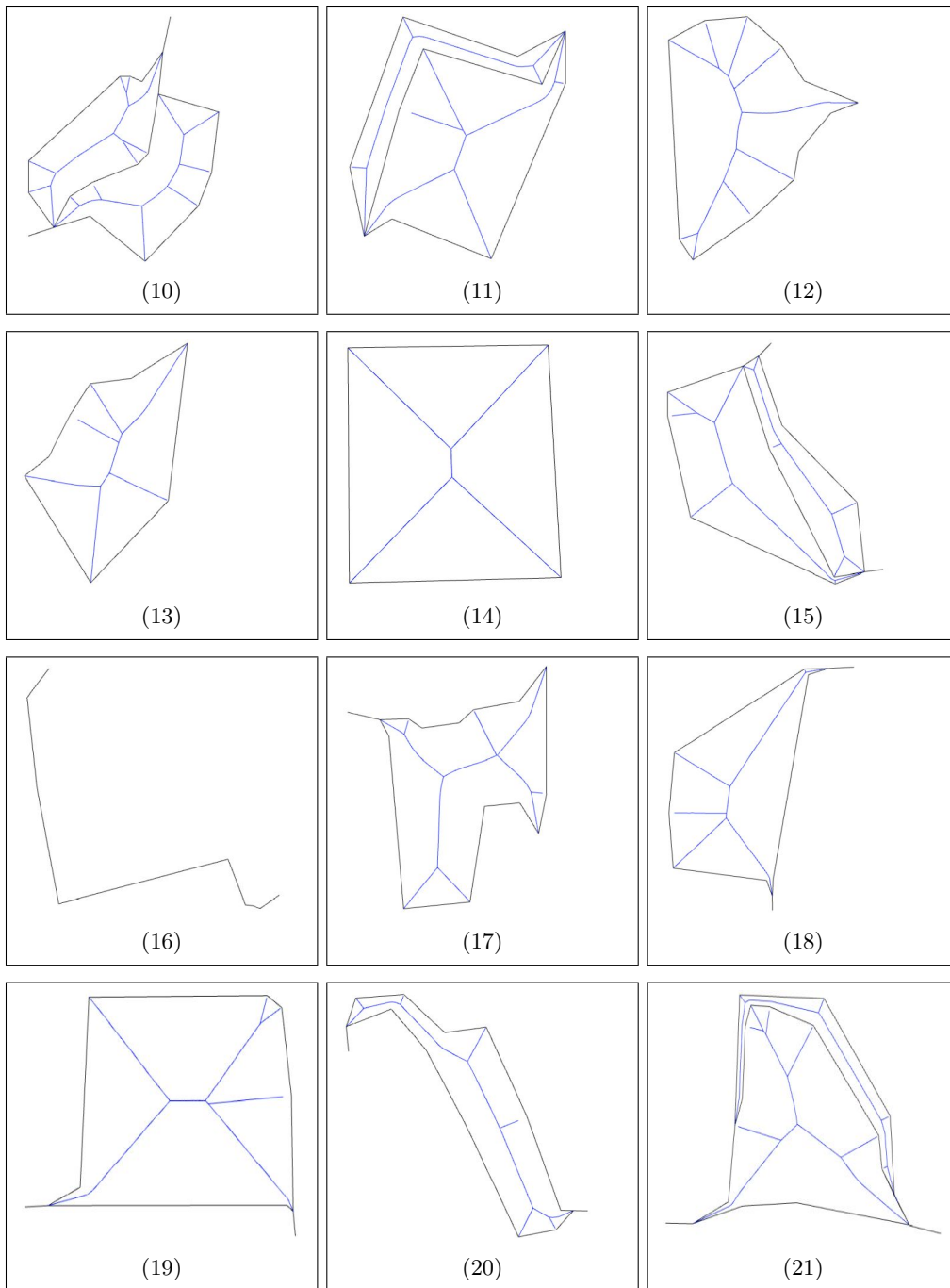
5 Results

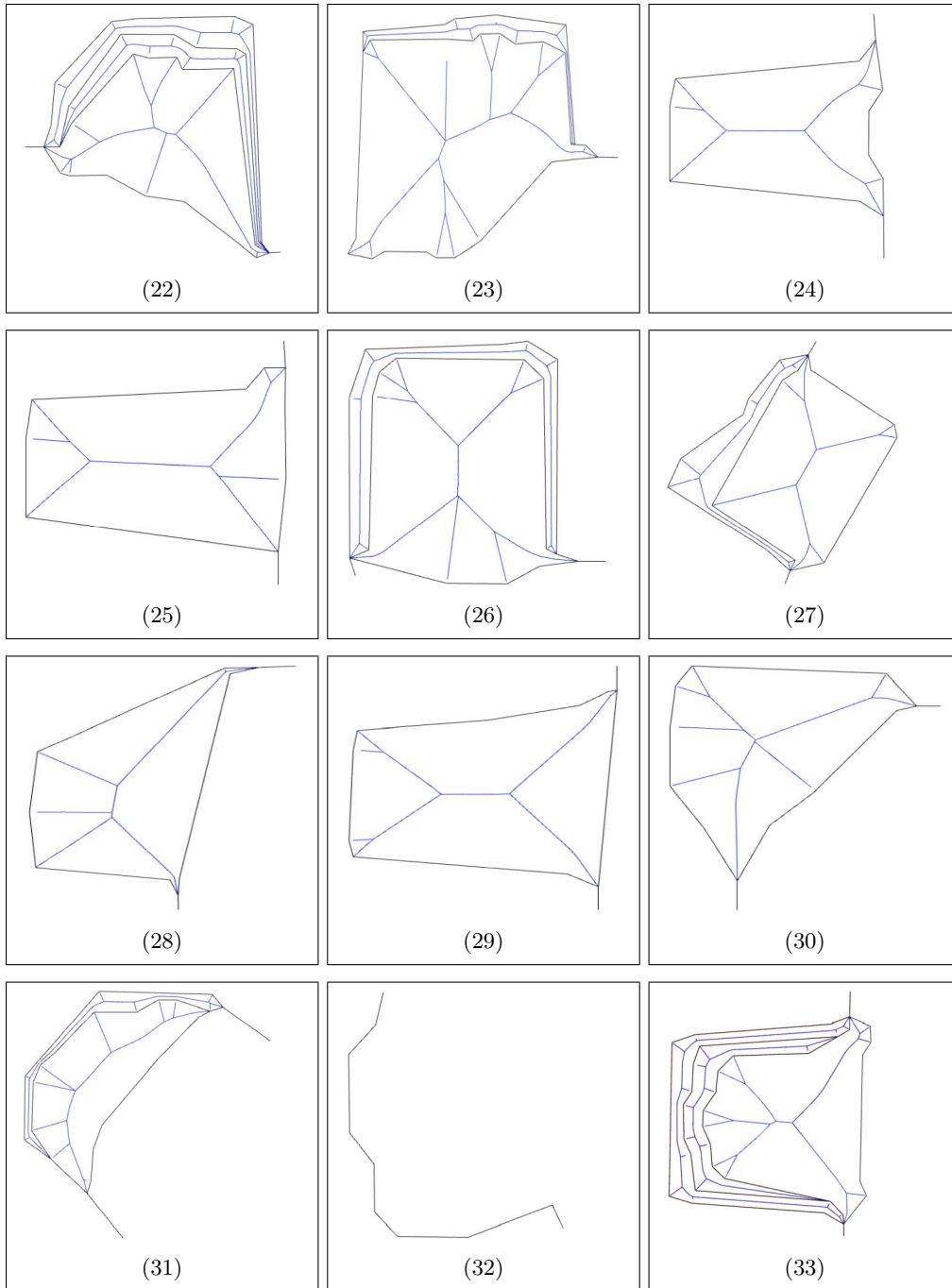
In this section the results for the geometrical properties and the FEM results are shown.

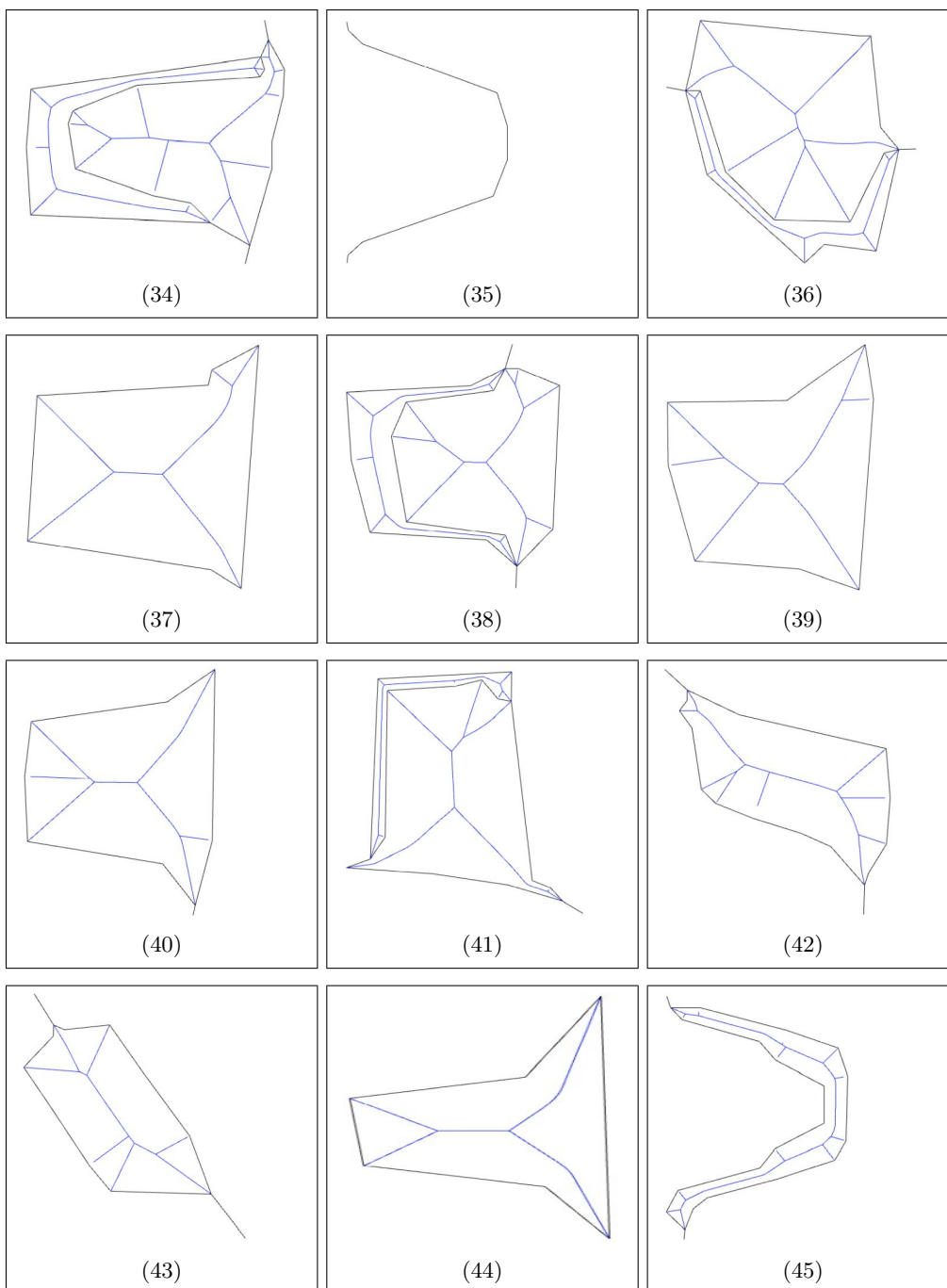
5.1 Cross-section geometries

Here every cross-section geometry from 4.1 with their corresponding medial axis are shown. These geometries were calculated and rendered in Rhino Grasshopper 4.4.1. The black lines correspond to the geometries outer circumference while the blue lines is the medial axis.









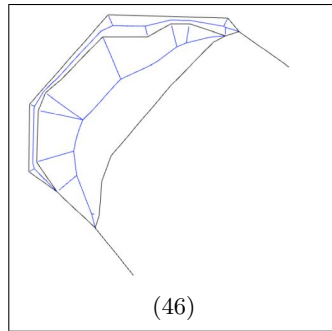


Figure 32: All 46 Cross-section geometries.

5.2 Geometrical parameter values

These are the values calculated in Rhino for each parameter of every geometry. Note that geometries 16, 32, and 35 have been left out from the results since they are not enclosed geometries.

Geometry No.	Circumference	Medial axis length	Area	M/C
1	380,8	676,8	2978,0	1,77
2	459,3	805,9	3459,6	1,75
3	398,8	697,9	3946,2	1,74
4	411,6	722,1	4745,5	1,75
5	470,1	831,5	4601,7	1,76
6	421,0	777,2	4688,7	1,84
7	354,8	688,1	3432,9	1,93
8	278,8	583,8	3708,1	2,09
9	310,5	725,1	5015,2	2,33
10	356,0	643,8	3576,2	1,80
11	461,6	790,5	5404,5	1,71
12	262,9	513,7	3780,7	1,95
13	240,3	395,3	3093,2	1,64
14	321,7	443,9	6440,6	1,38
15	380,4	591,4	3891,5	1,55
17	321,4	474,4	3515,4	1,47
18	275,0	376,7	3038,1	1,37
19	311,0	467,6	4791,4	1,50
20	307,5	368,2	2147,0	1,19
21	415,4	662,2	3061,3	1,59
22	670,2	1322,7	5384,7	1,97
23	415,8	925,9	5054,5	2,22
24	297,8	403,7	3684,1	1,35
25	302,4	436,2	4362,0	1,44
26	529,9	1011,2	6123,3	1,90
27	377,0	655,0	4023,5	1,73
28	402,5	653,7	5193,5	1,62
29	290,5	389,9	4197,5	1,34
30	273,3	462,8	3516,6	1,69
31	432,1	702,9	3060,3	1,62
33	615,4	1231,2	4941,2	2,00
34	467,6	895,5	4939,2	1,91
36	434,8	836,2	5486,2	1,92
37	328,7	457,5	5695,5	1,39
38	435,8	789,6	4687,1	1,81
39	319,1	498,3	5608,3	1,56
40	287,6	444,8	4198,5	1,54
41	444,0	708,2	4575,5	1,59
42	288,6	431,1	3041,8	1,49
43	257,2	376,5	2732,8	1,46
44	250,1	314,2	2171,9	1,25
45	344,1	417,7	1409,7	1,21
46	403,4	812,7	4323,5	2,01

Table 11: The calculated values for each parameter

5.3 Simulation results

Here the FEM results for every geometry are shown, and every geometry is shown with its corresponding specific energy absorption (SEA) and peak crush force (P_{max}) for every thickness.

Thickness	1 mm		2 mm		3 mm	
Geometry	SEA	P_{max} (N)	SEA	P_{max} (N)	SEA	P_{max} (N)
1	15,16	92033	14,95	205920	25,27	313529
2	12,52	108135	12,36	244850	20,91	377555
3	14,51	94598	14,39	210142	24,30	323636
4	14,00	97830	13,96	217053	23,59	334354
5	12,57	109154	12,43	239810	20,96	372635
6	13,71	101028	13,65	219730	23,16	339391
7	16,54	82474	16,42	176456	27,57	277124
8	20,95	64201	20,94	135635	35,00	214503
9	18,90	71840	18,83	149564	31,55	236047
10	16,43	82902	16,36	179231	27,44	279842
11	12,51	110919	12,42	239112	21,12	371199
12	22,24	62164	22,26	134765	37,18	211245
13	24,28	57025	24,33	123779	40,69	193181
14	18,05	80525	17,92	172771	30,21	265264
15	15,15	92793	15,13	198069	25,39	309706
17	18,11	78828	18,02	173836	30,295	266530
18	21,28	66249	21,34	139866	35,65	216775
19	19,13	74174	19,04	156620	32,027	246379
20	18,99	74911	18,97	161126	31,81	250527
21	14,75	93390	14,70	201378	24,67	312849
22	8,56	158759	8,491	341307	14,45	528069
23	13,73	100992	13,62	220785	23,03	339316
24	19,571	71427	19,46	155820	32,78	240157
25	19,26	73638	19,15	157970	32,21	245107
26	10,76	130314	10,61	274114	17,95	427522
27	15,33	89566	15,29	195609	25,80	30559
28	14,29	96452	14,28	211165	24,10	326680
29	20,02	70834	20,02	153584	33,42	239550
30	21,36	65675	21,36	139421	35,83	218103
31	14,81	92971	14,80	199493	24,78	306716
33	9,21	150867	9,11	327758	15,49	503896
34	12,17	113338	12,11	244709	20,41	380583
36	13,34	103162	13,26	221729	22,44	341977
37	17,69	80397	17,57	173963	29,60	270536
38	13,33	102344	13,22	222406	22,29	348344
39	18,23	77441	18,30	161735	30,57	252153
40	20,26	68715	20,34	150405	33,97	234160
41	13,11	106251	12,98	230624	21,87	359627
42	21,65	64662	21,71	135806	36,27	212767
43	22,87	61466	22,89	128414	38,25	200424
44	23,26	59824	23,16	130817	39,06	204674
45	17,03	80601	16,98	176610	28,48	274956
46	14,47	95184	14,29	208371	24,05	326878

Table 12: FEM results for each geometry and thickness

5.4 Correlation studies

In this section, the FEM results for peak crush force and SEA for every geometry are compared in order to determine the correlation between them and the four different parameters.

In table 13 the R^2 values for each thickness and every parameter compared to PCF is shown. While in table 14 the same values are shown but instead compared to the SEA.

Thickness (mm)	Circumference	Medial axis length	Area	M/C
1	0,9877	0,8659	0,2437	0,1967
2	0,9833	0,8557	0,223	0,1902
3	0,9853	0,8623	0,2262	0,1962
Average	0,9854	0,8613	0,231	0,1944

Table 13: Correlation R^2 values for peak crush force

Thickness (mm)	Circumference	Medial axis length	Area	M/C
1	0,9922	0,7978	0,2385	0,2054
2	0,9915	0,8157	0,2381	0,2053
3	0,9925	0,8178	0,2366	0,2072
Average	0,9921	0,8104	0,2377	0,206

Table 14: Correlation R^2 values for specific energy absorption

5.4.1 Circumference

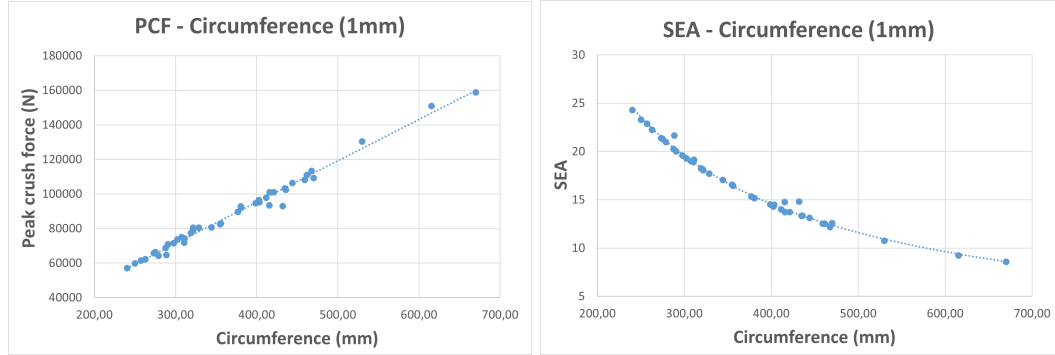


Figure 33: Peak crush force and SEA compared to circumference for 1 mm thickness.

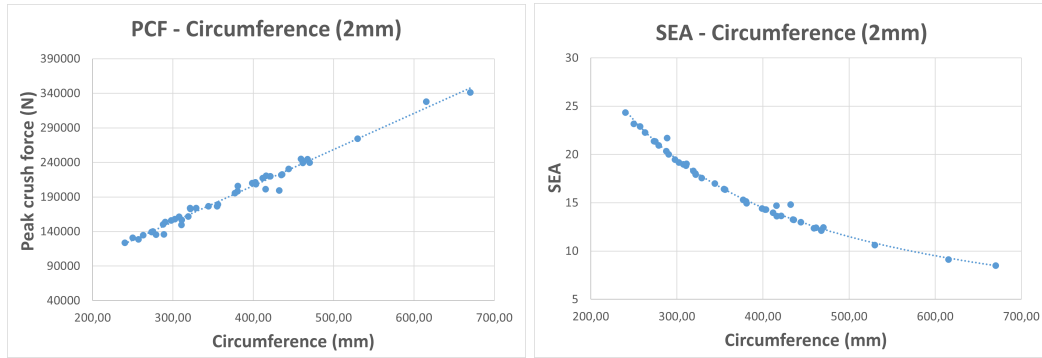


Figure 34: Peak crush force and SEA compared to circumference for 2 mm thickness.

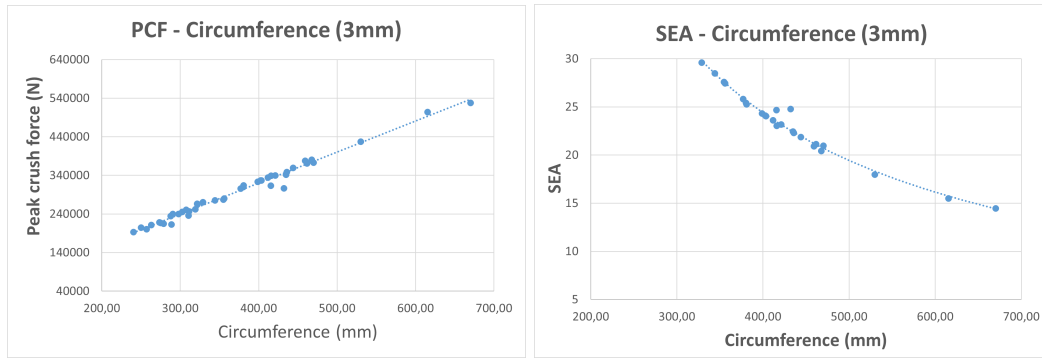


Figure 35: Peak crush force and SEA compared to circumference for 3 mm thickness.

5.4.2 Medial axis length

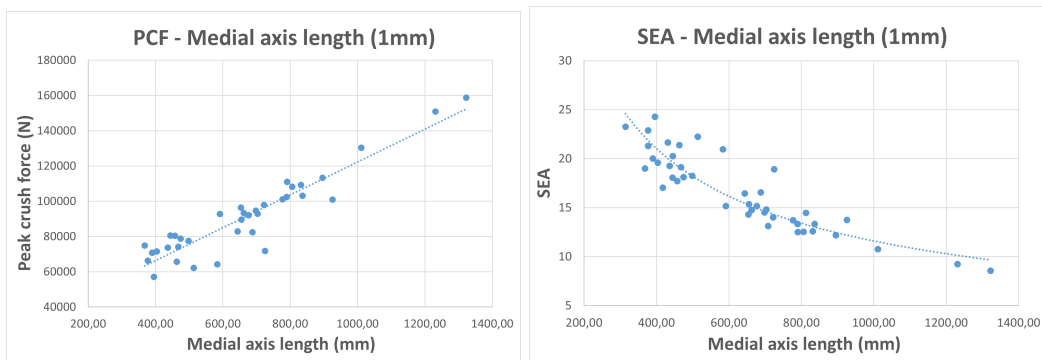


Figure 36: Peak crush force and SEA compared to medial axis length for 1 mm thickness.

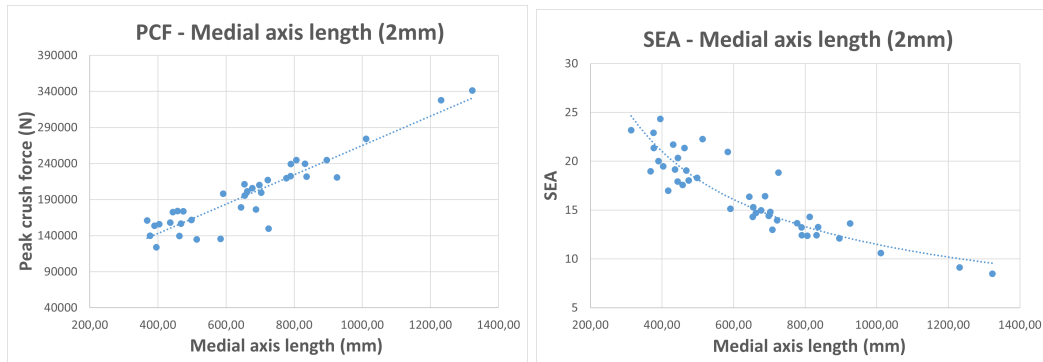


Figure 37: Peak crush force and SEA compared to medial axis length for 2 mm thickness.

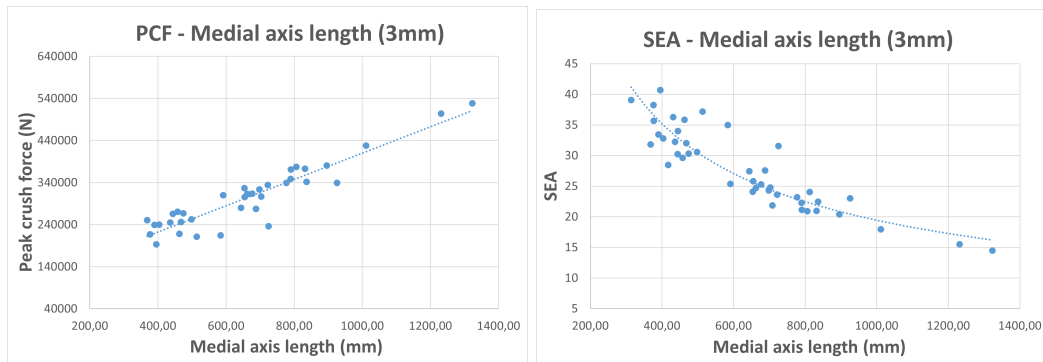


Figure 38: Peak crush force and SEA compared to medial axis length for 3 mm thickness.

5.4.3 Area

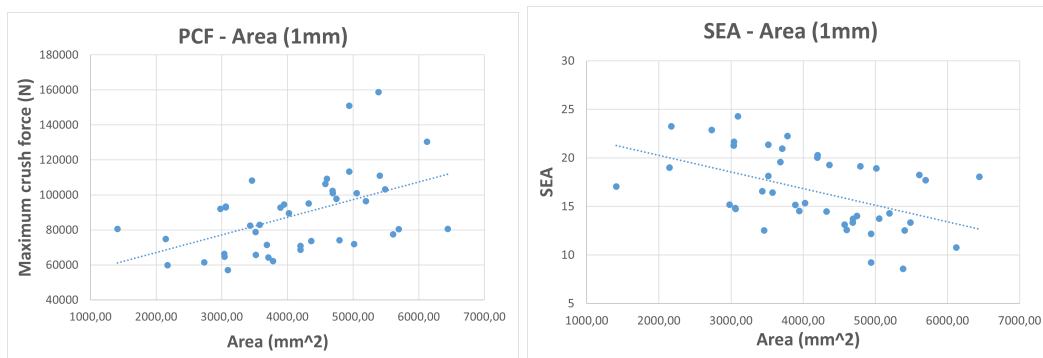


Figure 39: Peak crush force and SEA compared to area for 1 mm thickness.

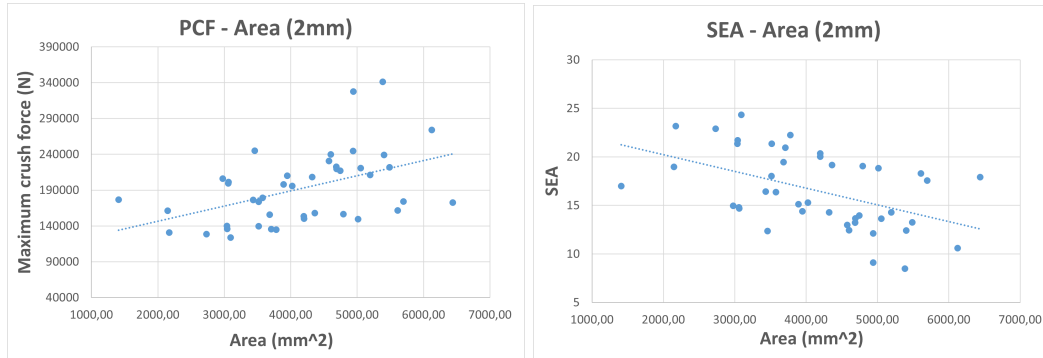


Figure 40: Peak crush force and SEA compared to area for 2 mm thickness.

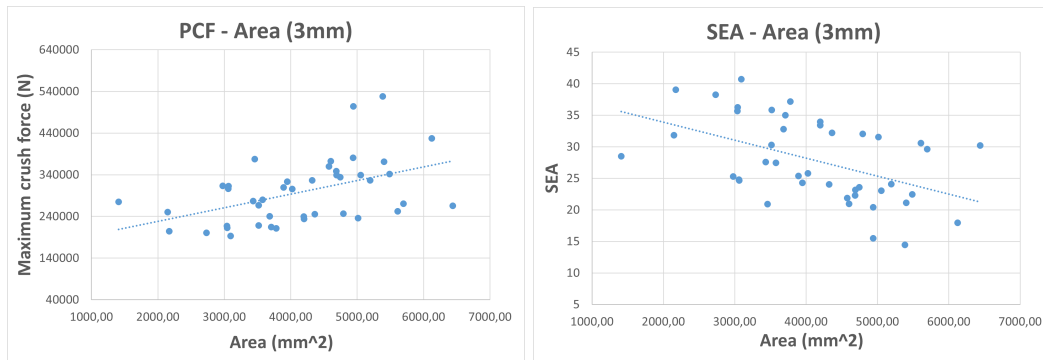


Figure 41: Peak crush force and SEA compared to area for 3 mm thickness.

5.4.4 M/C ratio

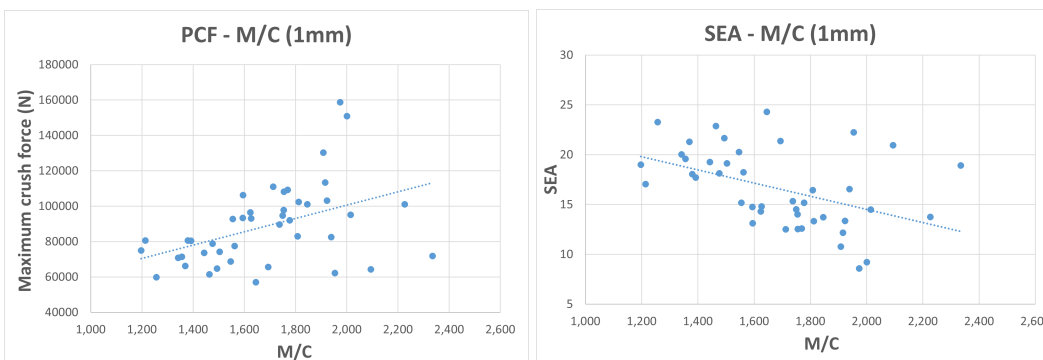


Figure 42: Peak crush force and SEA compared to the M/C ratio for 1 mm thickness.

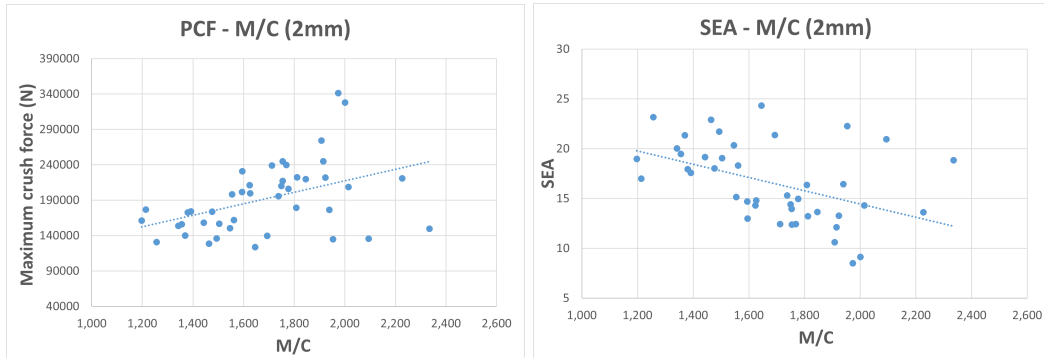


Figure 43: Peak crush force and SEA compared to the M/C ratio for 2 mm thickness.

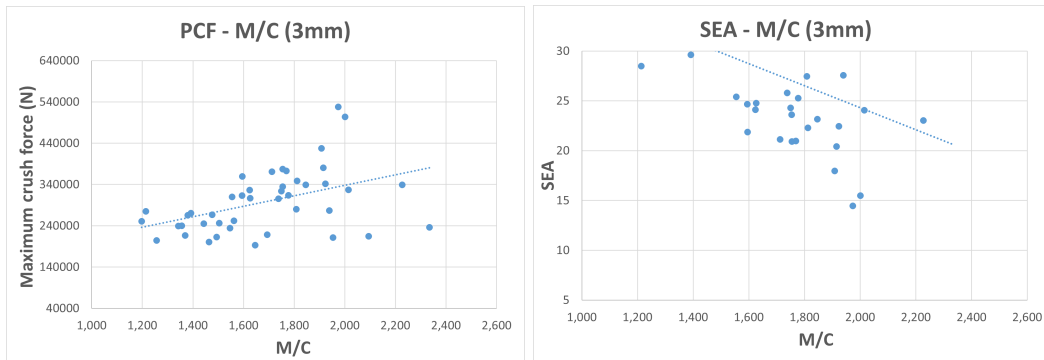


Figure 44: Peak crush force and SEA compared to the M/C ratio for 3 mm thickness.

6 Discussion

6.1 Research question 1

What methods and tools are used today to shorten the development lead time for thin-walled tubes?

In recent years the main producer of TWBs, the automobile industry, has moved away from physical tests and instead uses a variety of CAE tools to analyze their designs. These tools largely include the use of FEM simulations, not only in the final phases of development but also in the initial phases. This helps streamline the development process by not having to wait until the end in order to validate designs.

Additional methods used for shortening the development lead times are discussed in chapter 2 and include simplifying the FEM models or using genetic algorithms to optimize a TWBs cross-section before simulations.

6.2 Research question 2

What are the main challenges in the development process for thin walled tubes?

The use of FEM methods still presents many challenges, the main one being the large amount of processing power required, FEM crash simulations are some of the most complex nonlinear problems in structural mechanics. This leads to long simulation times possibly lasting for several days prolonging the development lead times.

Moreover, FEM models need to be validated in order to make sure they represent how energy-absorbing structures behave in reality. This leads to further prolonging the development process.

6.3 Research question 3

What types of methods can be developed to shorten the development lead time of thin walled tubes?

In our thesis, a method for predicting TWBs crashworthiness is investigated. Our method consists of parameterizing several cross-section geometries with 4 different parameters, circumference, medial axis length, area, and M/C ratio. These parameters are then compared to the FEM results of the corresponding tube geometry and analyzed for correlations.

6.4 Method/Results

Every geometrical cross-section geometry is shown in chapter 4.1 and their corresponding parameter values can be seen in table 11. These parameters were calculated in Rhino Grasshopper. The results from the FEM simulations can be seen in table 12.

The R^2 correlation values found when comparing circumference with PCF and SEA are

0,9854 (table 13) and 0,9921 (table 14) respectively. These R^2 values indicate a strong correlation between the circumference of a geometry and the crashworthiness metrics PCF and SEA. A weaker correlation was found when comparing with medial axis length, R^2 averages values of 0,8613 and 0,8104. No significant correlations were found between Area and medial length circumference ratio.

The most interesting parameter to discuss is the circumference, because of its strong correlations with peak crush force and SEA. A few different factors could be contributing to this behavior, the mass of the beam is directly proportional to the cross-section circumference, so the circumference correlations could also be described as mass correlations. Nevertheless, it is interesting to note that the circumference correlations indicate that if we know the circumference of the cross-sections we can accurately predict its crashworthiness no matter how different the actual geometries are. Although it's still important to note that the number of geometries tested was small and with a minor difference when it comes to length-to-width, ratios, leading to all the tubes buckling locally. If more geometries were tested with bigger length-to-width ratios they might start to buckle globally instead. Leading to their crashworthiness not being as easy to predict.

Our proposed method of assessing the crashworthiness of TWBs greatly shortens the validation process, a FEM simulation of a TWB took on average 30 minutes while the process for calculating the 4 different parameters only took a few seconds.

6.5 Further research

There are many areas where additional research could be conducted. Since the Abaqus code constructs geometries from points, an algorithm could be developed to construct random points, these points could be used to construct random geometries, based on predefined rules and tested for crashworthiness. By doing this, cases where our predictions don't apply, could be found and further studied.

Geometries with the same circumference could be constructed in order to see what effects the actual shape of the geometry has, here the medial axis and M/C ratio might be used to predict the crashworthiness in a more successful manner.

Since the correlation with circumference is so strong there might be some underlying link to some known physics concept. This might be the second moment of inertia since it's the only cross sectional parameter in Euler's buckling formula. Additional research could be done here to analyze the link between our results and the second moment of inertia.

Another thing that would be interesting to add except for more functions is a user interface (UI). This would make it easier to use and even people that have poor programming skills could use it. It would also be useful to create a better database so that different information could be stored and used in the script depending on what kind of simulations are needed.

7 Conclusion

The development of thin-walled tubes is a resource-intensive process, this thesis aims to shorten this process by predicting the TWBs crashworthiness before simulations are done. 43 different cross-section tube geometries that were extracted from a Toyota RAV4, are used. A method for automating tube crushing simulations in Abaqus was developed and used to simulate the geometries for their crashworthiness. The results from the FEM simulations were later compared to the 4 calculated parameters for each geometry. These 4 parameters were, circumference, medial axis length, area, and circumference medial axis length ratio. After the results were compared and analyzed for correlation with a simple regression model it was found that a geometries circumference and medial axis length are able to predict its crashworthiness. The area and circumference to medial axis ratio showed no ability in predicting the crashworthiness of the geometries. This result could be used to shorten the verification time for TWBs, leading to improvements in the development lead times of TWBs.

References

- [1] C. Gui, J. Bai, W. Zuo, Simplified crashworthiness method of automotive frame for conceptual design, *Thin-Walled Structures* 131 (2018) 324–335. doi:<https://doi.org/10.1016/j.tws.2018.07.005>. URL <https://www.sciencedirect.com/science/article/pii/S026382311731563X>
- [2] M. van der Seijs, *Experimental dynamic substructuring: Analysis and design strategies for vehicle development* (2016).
- [3] A. Baroutaji, M. Sajjia, A.-G. Olabi, On the crashworthiness performance of thin-walled energy absorbers: recent advances and future developments, *Thin-Walled Structures* 118 (2017) 137–163.
- [4] W. Zuo, J. Bai, Cross-sectional shape design and optimization of automotive body with stamping constraints, *International Journal of Automotive Technology* 17 (6) (2016) 1003–1011.
- [5] W. Abramowicz, N. Jones, Transition from initial global bending to progressive buckling of tubes loaded statically and dynamically, *International Journal of Impact Engineering* 19 (5) (1997) 415–437. doi:[https://doi.org/10.1016/S0734-743X\(96\)00052-8](https://doi.org/10.1016/S0734-743X(96)00052-8). URL <https://www.sciencedirect.com/science/article/pii/S0734743X96000528>
- [6] Z. Li, R. Chen, F. Lu, Comparative analysis of crashworthiness of empty and foam-filled thin-walled tubes, *Thin-Walled Structures* 124 (2018) 343–349. doi:<https://doi.org/10.1016/j.tws.2017.12.017>. URL <https://www.sciencedirect.com/science/article/pii/S0263823117309679>
- [7] D. E. Malen.p.cm, *Fundamentals of Automobile Body Structure Design*, SEA International, 2011.
- [8] A. Gupta, *Writer dependent handwriting synthesis*, Ph.D. thesis (07 2006).
- [9] W. Zuo, Y. Lu, X. Zhao, J. Bai, Cross-sectional shape design of automobile structure considering rigidity and driver’s field of view, *Advances in Engineering Software* 115 (2018) 161–167. doi:<https://doi.org/10.1016/j.advengsoft.2017.09.006>. URL <https://www.sciencedirect.com/science/article/pii/S0965997817307548>
- [10] A. Moghaddam, A. Kheradpisheh, M. Asgari, A basic design for automotive crash boxes using an efficient corrugated conical tube, *Proceedings of the Institution of Mechanical Engineers, Part D: Journal of Automobile Engineering* 235 (2021) 095440702199092. doi:<https://doi.org/10.1177/0954407021990921>.
- [11] D. G. Reinertsen, *The principles of product development flow: second generation lean product development*, Vol. 62, Celeritas Redondo Beach, 2009.
- [12] U. Sellgren, *Simulation-driven design: motives, means, and opportunities*, Ph.D. thesis, KTH (1999).
- [13] A. Maria, *Introduction to modeling and simulation*, *Winter Simulation Conference Proceedings*, (1997) 7–13.

-
- [14] H. C. Martínez León, J. A. Farris, G. Letens, Improving product development performance through iteration front-loading, *IEEE Transactions on Engineering Management* 60 (3) (2013) 552–565. doi:10.1109/TEM.2012.2228205.
- [15] B. Julien, D. Chamoret, S. Roth, I. Jean-Remy, S. Gomes, Knowledge based simulation driven design for crash applications, *International journal of mechanics and applications* 4 (09 2012). doi:10.5923/j.mechanics.20120205.01.
- [16] G. D'Al, Experimental and numerical investigation of static and dynamic axial crushing of circular aluminum tubes, *Thin-Walled Structures* 42 (2004) 1103–1137. doi:<https://doi.org/10.1016/j.tws.2004.03.001>.
- [17] Y. Xiang, Q. Wang, Z. Fan, H. Fang, Optimal crashworthiness design of a spot-welded thin-walled hat section, *Finite Elements in Analysis and Design* 42 (10) (2006) 846–855. doi:<https://doi.org/10.1016/j.finel.2006.01.001>.
URL <https://www.sciencedirect.com/science/article/pii/S0168874X06000102>
- [18] T. Belytschko, W. K. Liu, B. Moran, K. Elkhodary, *Nonlinear finite elements for continua and structures*, John wiley & sons, 2014.
- [19] S. Esmaeili-Marzdashti, S. Pirmohammad, S. Esmaeili-Marzdashti, Crashworthiness analysis of s-shaped structures under axial impact loading, *Latin American Journal of Solids and Structures* 14 (2017) 743–764.
- [20] K. C. Shin, J. J. Lee, K. H. Kim, M. C. Song, J. S. Huh, Axial crush and bending collapse of an aluminum/gfrp hybrid square tube and its energy absorption capability, *Composite Structures* 57 (1) (2002) 279–287. doi:[https://doi.org/10.1016/S0263-8223\(02\)00094-6](https://doi.org/10.1016/S0263-8223(02)00094-6).
URL <https://www.sciencedirect.com/science/article/pii/S0263822302000946>
- [21] T. Tran, S. Hou, X. Han, W. Tan, N. Nguyen, Theoretical prediction and crashworthiness optimization of multi-cell triangular tubes, *Thin-Walled Structures* 82 (2014) 183–195. doi:<https://doi.org/10.1016/j.tws.2014.03.019>.
URL <https://www.sciencedirect.com/science/article/pii/S02638223114001128>
- [22] W. Zuo, Y. Lu, X. Zhao, J. Bai, Cross-sectional shape design of automobile structure considering rigidity and driver's field of view, *Advances in Engineering Software* 115 (2018) 161–167. doi:<https://doi.org/10.1016/j.advengsoft.2017.09.006>.
URL <https://www.sciencedirect.com/science/article/pii/S0965997817307548>
- [23] E. Osslander, T. Koepsell, B. McKnight, Crash fatality risk and unibody versus body-on-frame structure in suvs, *Accident; analysis and prevention* 70C (2014) 267–272. doi:10.1016/j.aap.2014.03.019.
- [24] Y. Türe, C. Türe, An assessment of using aluminum and magnesium on co2 emission in european passenger cars, *Journal of Cleaner Production* 247 (2020) 119120. doi:<https://doi.org/10.1016/j.jclepro.2019.119120>.
URL <https://www.sciencedirect.com/science/article/pii/S0959652619339903>
- [25] J. Hirsch, Aluminium in innovative light-weight car design, *MATERIALS TRANSACTIONS* 52 (5) (2011) 818–824. doi:10.2320/matertrans.L-MZ201132.

- [26] B. Broberg, J. Carlsson, G. Hedner, H. Johansson, Handbok och formelsamling i hållfasthetslära, Institutionen för hållfasthetslära KTH, 2016.
- [27] What is finite element mesh refinement? (2016 (accessed 05-22, 2022)).
URL <https://www.simscale.com/docs/simwiki/fea-finite-element-analysis/what-is-fea-finite-element-analysis/>
- [28] What is fea — finite element analysis? (2021 (accessed 05-22, 2022)).
URL <https://www.comsol.com/multiphysics/mesh-refinement>
- [29] Abaqus simulia (2009 (accessed 05-25, 2022)).
URL <https://classes.engineering.wustl.edu/2009/spring/mase513/abaqus/docs/v6.6/books/gsx/default.htm?startat=ch02.html>
- [30] Simulia, Getting started with Abaqus: Interactiv Edition (9.3.2) (2021 (accessed 05-14, 2022)).
URL <http://130.149.89.49:2080/v6.14/books/gsa/default.htm>
- [31] What is python? executive summary ((accessed 05-20, 2022)).
URL <https://www.python.org/doc/essays/blurb/>
- [32] D. Lee, Medial axis transformation of a planar shape, IEEE transactions on pattern analysis and machine intelligence 4 (1982) 363–9. doi:10.1109/TPAMI.1982.4767267.
- [33] Abaquscode (2022 (2022-08-08)).
URL <https://github.com/BlomDaniell/Daniel-Andreas-Master-Thesis.git>
- [34] M. K. Thompson, J. M. Thompsen, Ansys mechanical apdl for finite element analysis (2017).
- [35] Abaqus simulia (2017 (accessed 06-08, 2022)).
URL <https://abaqus-docs.mit.edu/2017/English/SIMACAEMODRefMap/simamod-c-rigidsurf.htm>
- [36] Abaqus simulia (2017 (accessed 06-08, 2022)).
URL <https://abaqus-docs.mit.edu/2017/English/SIMACAEMODRefMap/simamod-c-rigidoverview.htm>
- [37] Abaqus simulia (2017 (accessed 06-08, 2022)).
URL <https://abaqus-docs.mit.edu/2017/English/SIMACAEEXCRefMap/simaexc-c-parallelexecution.htm>